JOURNAL OF GEOPHYSICAL RESEARCH, VOL. 100, NO. C7, PAGES 13,345–13,367, JULY 15, 1995

# Scales of variability of bio-optical properties as observed from near-surface drifters

Mark R. Abbott,[1] Kenneth H. Brink,[2] C. R. Booth,[3] Dolors Blasco,[4]
Mark S. Swenson,[5] Curtiss O. Davis,[6] and L. A. Codispoti[7]

**Abstract.** A drifter equipped with bio-optical sensors and an automated water sampler was deployed in the California Current as part of the coastal transition zone program to study the biological, chemical, and physical dynamics of the meandering filaments. During deployments in 1987 and 1988, measurements were made of fluorescence, downwelling irradiance, upwelling radiance, and beam attenuation using several bio-optical sensors. Samples were collected by an automated sampler for later analysis of nutrients and phytoplankton species composition. Large-scale spatial and temporal changes in the bio-optical and biological properties of the region were driven by changes in phytoplankton species composition which, in turn, were associated with the meandering circulation. Variance spectra of the bio-optical parameters revealed fluctuations on both diel and semidiurnal scales, perhaps associated with solar variations and internal tides, respectively. Offshore, inertial-scale fluctuations were apparent in the variance spectra of temperature, fluorescence, and beam attenuation. Although calibration samples can help remove some of these variations, these results suggest that the use of bio-optical data from unattended platforms such as moorings and drifters must be analyzed carefully. Characterization of the scales of phytoplankton variability must account for the scales of variability in the algorithms used to convert bio-optical measurements into biological quantities.

## 1. Introduction

Satellite observations of ocean color provide a unique view of the large-scale patterns of phytoplankton pigment in the upper ocean. Coupled with increasingly sophisticated numerical models, there is now the potential to study basin-scale and global-scale biogeochemical processes in the ocean in greater detail than before. However, obstacles remain, especially in the parameterization of the unresolved scales. Similar problems confront models of ocean physics. For example, the parameterization of small-scale turbulence and diffusion significantly affects the large-scale patterns of heat flux [*Bryan*, 1987]. The characterization of small-scale variability is also necessary for optimal interpolation of sparse data sets. *Chelton and Schlax* [1991] used estimates of the variance spectrum to derive optimal estimates of mean fields for irregularly sampled time series. They used a sequence of coastal zone color scanner (CZCS) imagery to show that composite averages provide little information where there are long gaps in the series. Using maps of field measurements, *Denman and Freeland* [1985] estimated the structure functions of chlorophyll and a set of physical variables to produce objective maps. Thus both parameterization for models and optimal estimates for temporal and spatial fields rely on estimates of the subgrid-scale variability to map the larger-scale fields of interest.

Such small-scale variability is more than merely a nuisance for sampling and modeling. As phytoplankton growth rates respond on scales of a day or less (and hence on spatial scales of tens of kilometers), this subgrid-scale is likely the focus of physical/biological coupling [*Denman and Powell*, 1984; *Harris*, 1986; *Abbott*, 1993]. As these scales are difficult to observe, it is essential that we begin to characterize this variability sufficiently to derive statistically robust fields and models at larger scales.

Bio-optical measurements have been used for decades as surrogates for direct measurements of biological properties [*Zaneveld*, 1989; *Smith et al.*, 1991; *Marra*, 1995]. With improvements in data storage, batteries, and sensor design, routine bio-optical measurements can be made from unattended platforms such as moorings and drifters [*Dickey*, 1991]. Such observation strategies now allow the study of processes that were previously difficult to resolve using conventional shipboard techniques [*Dickey et al.*, 1991; *Smith et al.*, 1991; *Marra*, 1995]. With their ability to resolve small-scale variability, these strategies will allow us to derive statistics necessary for techniques such as optimal interpolation.

During the spring/summer upwelling season, large meanders are apparent in the California Current [*Strub et al.*, 1991]. Inshore of these meanders, cold water is present near the surface and is characterized by high nutrient and chlorophyll concentrations. The coastal transition zone (CTZ) program was designed to characterize the physical, biological, and chemical dynamics of these meanders or filaments [*Brink and Cowles*, 1991]. Using an array of bio-optical sensors and automated water samplers, a drifter (drogue depth 13 m) was deployed once in 1987 and once in 1988. The water-following characteristics of this drifter should allow separation of temporal variability from spatial variability [*Niiler et al.*, 1987; *Paduan and Niiler*, 1990; *Brink et al.*, 1991; *Swenson et al.*, 1992], although vertical water movements will

[1]College of Oceanic and Atmospheric Sciences, Oregon State University, Corvallis.
[2]Woods Hole Oceanographic Institution, Woods Hole, Massachusetts.
[3]Biospherical Instruments, Incorporated, San Diego, California.
[4]Rimouski, Quebec, Canada.
[5]Atlantic Oceanographic and Meteorological Laboratory, NOAA, Miami, Florida.
[6]Naval Research Laboratory, Washington, D.C.
[7]Office of Naval Research, Arlington, Virginia.



Paper number 94JC02457.
0148-0227/95/94JC-02457$05.00

appear as temporal variations because the instruments are drogued at a constant depth. This meandering region is the site of relatively large vertical excursions, of the order of several tens of meters per day [*Washburn et al.*, 1991; *Kadko et al.*, 1991; *Swenson et al.*, 1992]. Thus estimates of the timescales of variability will include the scales of vertical motion as well as the scales associated with bio-optical changes in a particular water mass.

We compared several methods to derive biological properties such as chlorophyll concentration and primary productivity from the basic bio-optical signals. Although we were not able to derive estimates of absolute error, we were able to estimate the relative variability between the different methods on timescales of days. There were also considerable differences between the two deployments in the bio-optical properties of the phytoplankton which were apparent in these functional relationships. We suspect that these are largely driven by shifts in species composition which affect the observed bio-optical properties.

We use standard time series techniques to study the characteristic scales of variability. These results are compared with measurements of the physical environment to estimate the degree of coupling between physical and bio-optical variability. There is strong interaction between physical forcing and bio-optical properties at a wide range of timescales. Future sampling programs, especially those relying on satellite remote sensing, must take such small-scale variability into account when scaling up to large-scale models.

## 2. Sampling Techniques and the Physical Environment

The drifter used in this study has been described by *Niiler et al.* [1987], *Paduan and Niiler* [1990], and *Swenson et al.* [1992]. The bio-optical instrumentation included a Biospherical Instruments MER-2020, a SeaTech 25-cm beam transmissometer, and a SeaTech strobe fluorometer. Table 1 shows the variables that were recorded. An automated water sampler [*Friederich et al.*, 1986] was used to collect samples every 12 hours for later nutrient and phytoplankton analyses. The bio-optical sampler was placed at 8.5 m depth, and the water sampler was at 17.5 m. Bio-optical samples were collected every 4 min in the 1988 deployment after averaging for 45 s (We incorrectly stated in the work by *Abbott et al.* [1990] that the sampling interval was every 4 min; it was actually 8 min in 1987. This error does not affect any of the figures or analyses in that paper.) In 1988, samples were collected adjacent to the drifter at noon every day for shipboard analysis. Water samples were collected from the ship only at the beginning and end of the 1987 deployment. These samples were used to estimate chlorophyll concentrations using standard extraction methods.

**Table 1. Variables Recorded on Biospherical Instruments MER-2020 Spectroradiometer**

| Variable | Description |
|---|---|
| Downwelling irradiance, nm | 410, 441, 488, 520, 560 |
| Upwelling radiance, nm | 410, 441, 488, 520, 683 |
| Other variables | strobe fluorescence, beam transmission, temperature, depth |
| Housekeeping variables | time, tilt, ground voltage, battery voltage |

In both years the drifter was deployed near an upwelling center at the nearshore end of a filament. The drifters were tracked via the Argos system. The two drifters followed the main axis of the filament offshore. Figures 1a and 1b show the drifter tracks from 1987 and 1988. In both years the drifters started nearshore, off Point Arena, and proceeded in a southward direction offshore. Both drifters stayed near the cold core of the meandering filament. The instrumented drifters tracked the water motion as well as the uninstrumented drifters [*Swenson et al.*, 1992]. During both deployments the winds were generally southward in the range of 7 to 15 m/s.

Figure 2 shows a spline fit to the drifter positions in 1988 compared with the geopotential anomaly [*Huyer et al.*, 1991]. When compared with a similar figure from the 1987 deployment [*Abbott et al.*, 1990, Figure 4], it is apparent that the 1988 deployment more nearly sampled the core of the meander. Both *Kosro et al.* [1991] and *Huyer et al.* [1991] showed that acoustic Doppler current profiler (ADCP) maps of the velocity field reproduced the patterns in the circulation observations derived from conductivity-temperature-depth (CTD) measurements. In 1987 the drifter tended to be inshore of the high-velocity portion of the meander. The jet appears to have been stronger in 1988, based on estimates of the geopotential anomaly [*Huyer et al.*, 1991; *Kosro et al.*, 1991]. In the Point Arena region the filament was much narrower and more sharply defined than it was in 1987. The deployment in 1988 took place as the filament was oriented primarily offshore [*Huyer et al.*, 1991; *Chavez et al.*, 1991] as in 1987. However, shortly after this deployment, the offshore flow apparently decreased and the filament became oriented alongshore [*Huyer et al.*, 1991].

Figures 3a, 3b, and 3c show time series of temperature, strobe fluorescence, and downwelling scalar irradiance $E_0$ photosynthetically active radiation (PAR), respectively, from the 1988 deployment. Plots of these variables from 1987 are given by *Abbott et al.* [1990]. In both years the patterns of fluorescence and temperature were in general inversely related, as expected for upwelling regions [e.g., *Hood et al.*, 1990]. Temperature increased about 2°C in 1987 and about 3°C in 1988. As noted by *Abbott et al.* [1990], much of this increase was the result of convergence of warmer water along the path of the drifter in 1987, associated with a net downwelling of the surface water. Similar processes occurred in 1988, as *Swenson et al.* [1992] estimated that surface heating was in the range of 0.15° to 0.3°C/d, considerably less than the temperature change observed by the drifter.

We compared the horizontal transect obtained by the drifter with vertical sections of chlorophyll, temperature, and salinity, derived from the vertical profiles made at noon each day of the 1988 deployment next to the drifter (Figures 4a, 4b, and 4c). These show the strong front in temperature that occurred approximately 70 km along the drifter track on day 189 (Figure 4a). The sections also show the tendency for the nearshore waters which are characterized by low temperatures and high chlorophyll to subduct as they move offshore [*Washburn et al.*, 1991].

Figure 5 is the concentration of nitrate + nitrite (N+N) for the 1988 deployment. The pattern and absolute values of N+N are similar to the results from the 1987 deployment [*Abbott et al.*, 1990]. Although N+N disappeared at nearly the same rate as it did in the 1987 deployment, much of this change may have been the result of changes in water masses as the drifter crossed isopycnals (Figure 2) or vertical water motions. *Swenson et al.* [1992], using a vorticity budget method, calculated that there were was downwelling on day 187 (approximately 12 m/d), upwelling on

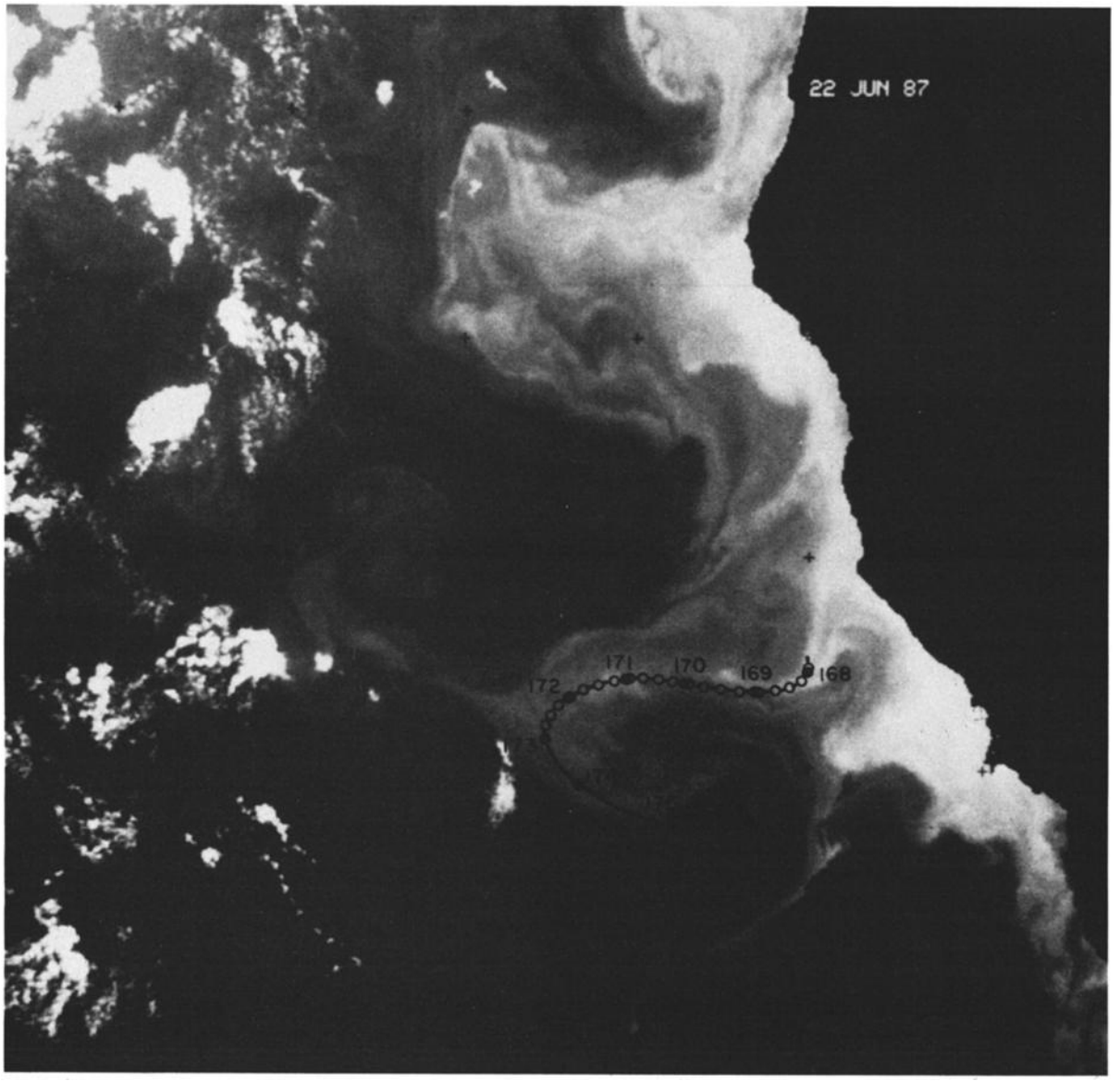


**Figure 1a.** Drifter path from 1987 superimposed over advanced very high resolution radiometer (AVHRR) image of sea surface temperature from *Abbott et al.* [1990].

day 188 (approximately 7 m/d), and downwelling on day 189 (approximately 8 m/d).

## 3. Methods and Results

### Chlorophyll Estimates

Our first objective was to compare different methods for converting bio-optical data into estimates of chlorophyll concentration. Part of this comparison was an assessment of the time and space scales of variation of algorithm performance. For example, were a particular set of parameters constant along the length of the drifter track or did they vary from water mass to water mass? As more observations are made remotely (e.g., from satellites or unattended moorings), the choice of algorithms becomes more critical. We must understand the total performance of the algorithm which includes both estimates of root-mean-square (rms) error as well as how its performance changes over time.

The first method converted the strobe fluorometer data using the chlorophyll extractions that were collected at the beginning and end of the deployment in 1987 and on a daily basis in 1988. Clearly, this method should be less accurate in 1987 than 1988. Numerous papers have appeared in recent years discussing the problems associated with calibration of fluorometers; in this experiment we assumed that the temporal/spatial scale of changes in fluorescence per unit chlorophyll was larger than the temporal/spatial scales over which we collected calibration samples. This is not a robust assumption as fluorescence/chlorophyll can change rapidly for a variety of physiological reasons [*Kiefer and Reynolds*, 1992].

The Sun-stimulated fluorescence method was based on the model described by *Kiefer et al.* [1989] and *Chamberlin et al.* [1990]. Although this method is relatively new, it does show promise, particularly in the estimation of primary productivity. *Kiefer et al.* [1989] discuss several reasons why the technique

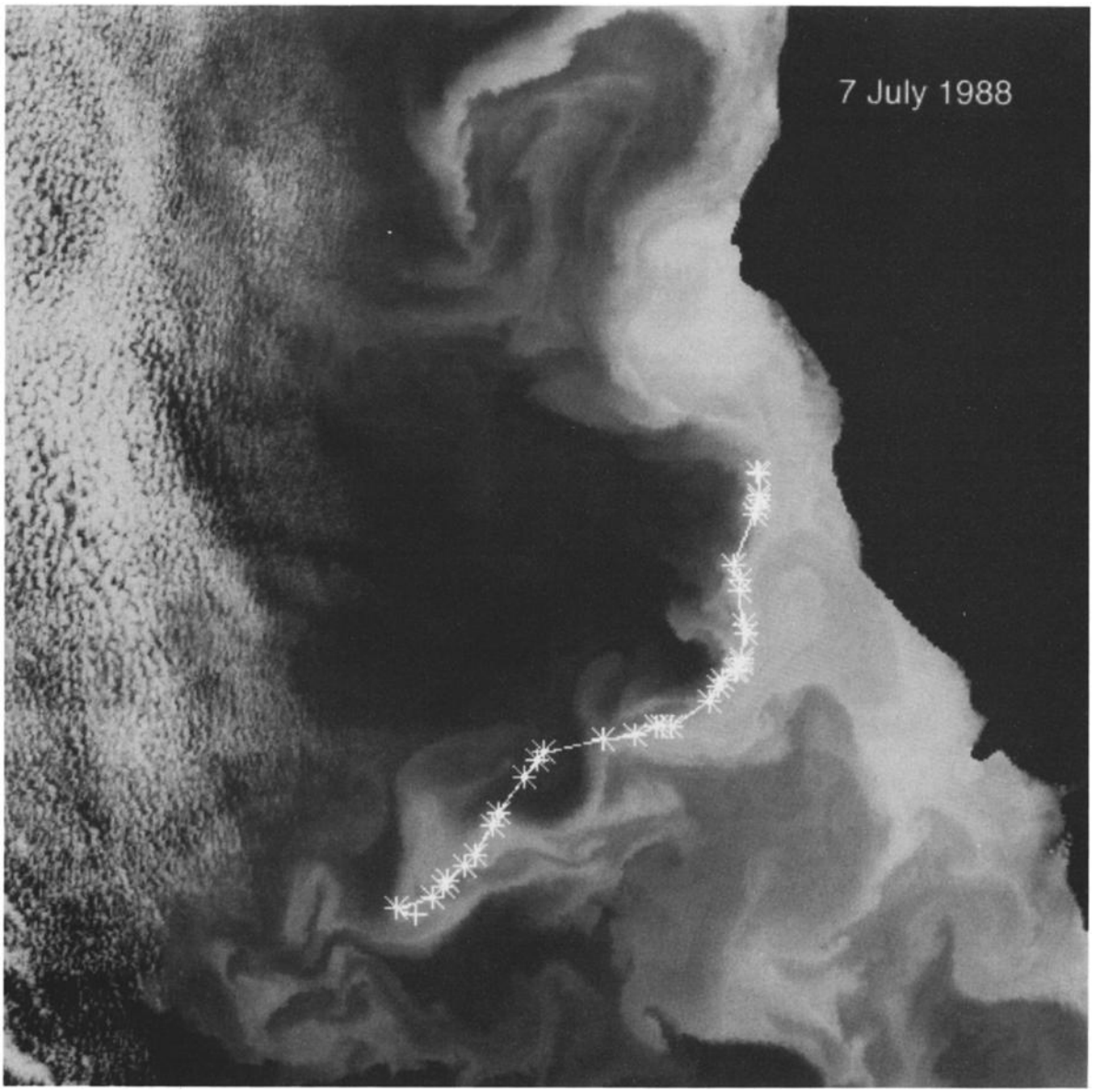


**Figure 1b.** Drifter path from 1988 superimposed over an AVHRR image of sea surface temperature.

should work better for estimates of primary productivity rather than chlorophyll concentration. The flux of Sun-stimulated fluorescence $F_f$ was calculated as follows:

$$F_f = 4\pi[k(\mathrm{PAR}) + a(\mathrm{Chl})] \times L_u(\mathrm{Chl}) \quad (1)$$

where $k$(PAR) is the diffuse attenuance for scalar irradiance between 400 and 700 nm [*Kiefer et al.*, 1989], $a$(Chl) is the total absorption coefficient, and $L_u$(Chl) is the spectrally integrated radiance of a chlorophyll-like substance. The $4\pi$ term is a geometric constant that transforms the radiance to a volume emission (with units of steradians, not $\mathrm{str}^{-1}$ as described by *Chamberlin et al.* [1990]). $F_f$ has units of nanoeinsteins per cubic meter per second and was converted to chlorophyll as

$$\mathrm{Chl} = \frac{F_f}{E_o(\mathrm{PAR}) \times \phi_f \times {}^{o}a_c(\mathrm{PAR})} \quad (2)$$

where $E_o$(PAR) is the downwelling scalar irradiance between 400 and 700 nm, $\phi_f$ is the quantum yield of fluorescence, and ${}^{o}a_c$ is the specific absorption coefficient of phytoplankton.

*Kiefer et al.* [1989] and *Kiefer and Reynolds* [1992] discuss the limitations of this approach. Specifically, the fluorescence signal may be confounded by the presence of other pigments. The quantum yield of fluorescence will change from species to species and depend on physiological state. Lastly, the specific absorption coefficient will not be constant.

In (1) we followed *Kiefer et al.* [1989] and assumed that $k$(PAR) + $a$(Chl) ≈ 0.52. This assumption works fairly well in waters where Chl < 2.0 $\mathrm{mg/m^3}$, a condition that was not always met in the study area. Assuming other parameters remain constant, this will result in an underestimate of chlorophyll concentrations in regions with Chl > 2.0 $\mathrm{mg/m^3}$.

$E_o$(PAR) was based on a linear regression of the downwelling irradiance at 520 nm, $E_d$(520), using

$$E_o(\mathrm{PAR}) = -0.0011 + 0.00245 \times E_d(520) \quad (3)$$

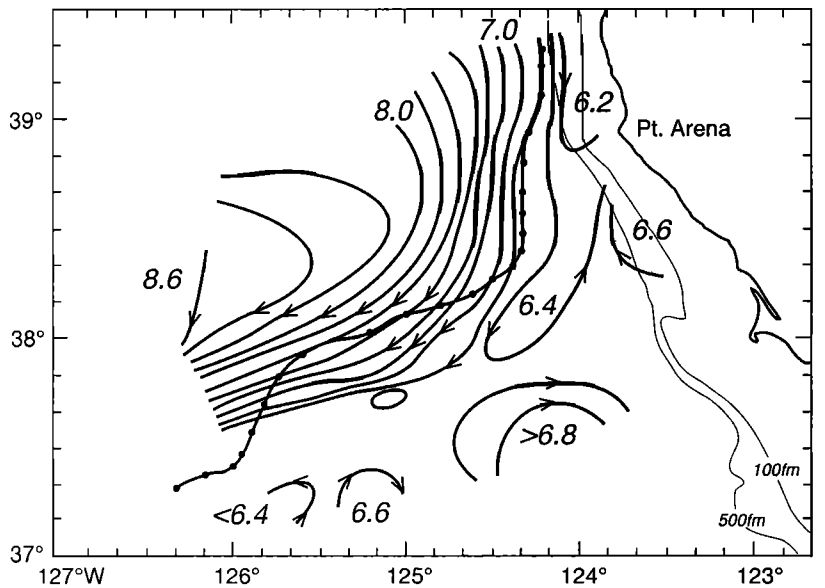


**Figure 2.** Path of 1988 drifter overlain on geopotential anomaly from the July 6–12 cruise (year days 188–194). Geopotential anomaly is from *Huyer et al.* [1991] and is calculated at 50 dbar relative to 500 dbar.

This is based on observations which show that downwelling radiance at 520 nm is only weakly affected by pigment concentration [*Gordon et al.*, 1988]. We compared this method with an estimate of the integrated radiance between 400 and 700 nm using the full spectroradiometric data. The correlation between the two estimates was 0.9996.

We used beam attenuation measurements to estimate chlorophyll by converting the raw transmissometer data to beam attenuation using the methods of *Bartz et al.* [1978]. We used the equations of *Bishop* [1986], where

$$\mathrm{SPM} = (c - c_w)/k \qquad (4)$$

In (4), SPM is suspended particulate matter, $c$ is the beam attenuation coefficient, $c_w$ is the beam attenuation resulting from pure water (assumed to be 0.358), and $k$ is an empirical coefficient relating beam attenuation to SPM. On the basis of *Bishop*'s [1986] data, we used $k = 1.15 \times 10^{-3}$. Following *Bishop* [1986], we assumed that approximately 25% of the SPM was carbon. We then converted this carbon estimate to chlorophyll, using a carbon:chlorophyll ratio of 60. As the beam transmissometer failed in the 1988 deployment, we present results only from 1987.

The beam attenuation method has several assumptions that may not be robust in our study area. *Bishop* [1986] shows that the relationship between attenuation and SPM can vary considerably

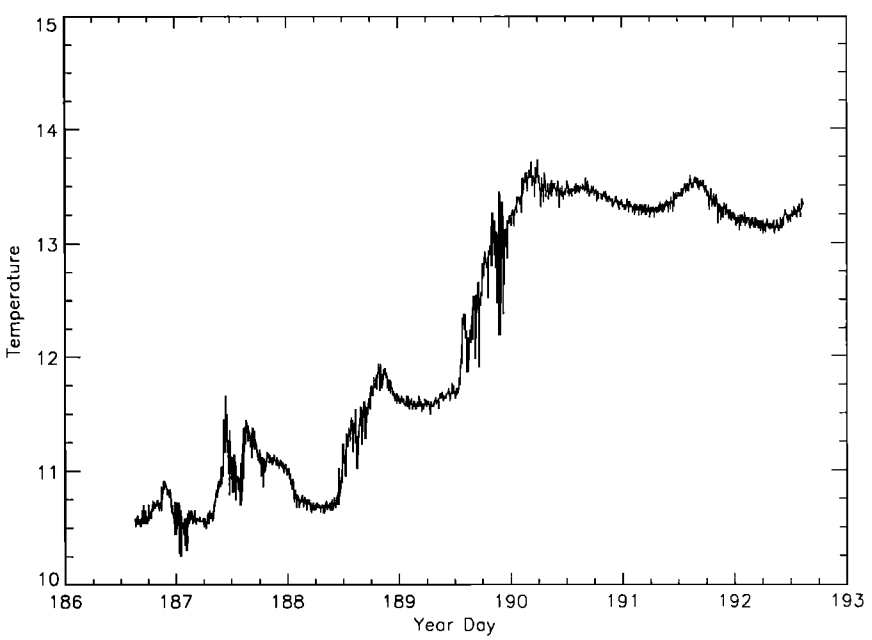


**Figure 3a.** Time series of temperature (in degrees Celsius) from the 1988 deployment.

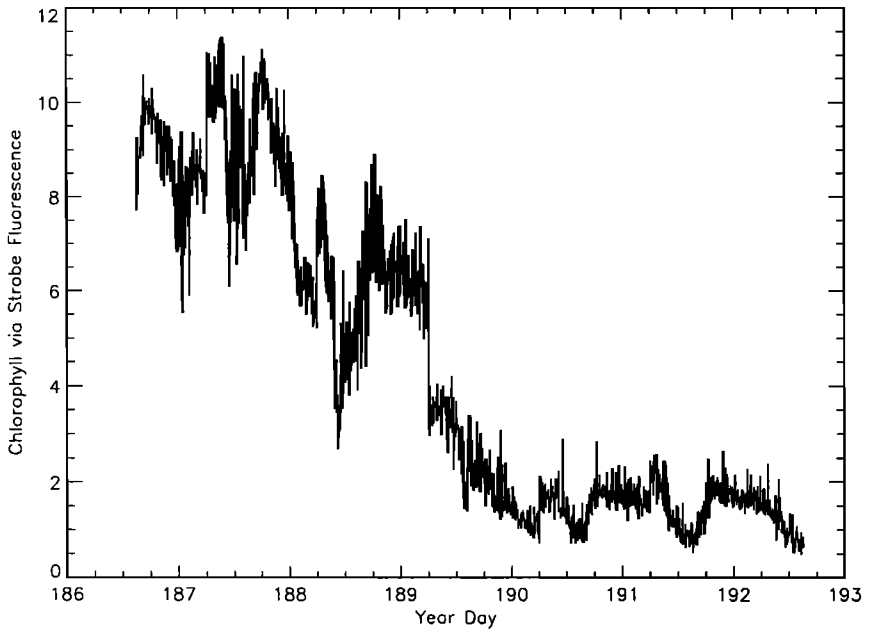


**Figure 3b.** Same as Figure 3a, but for strobe fluorescence.

depending on the oceanographic regime, particularly as one moves from coastal to oceanic regions. *Bishop* [1986] shows that errors can range from 20 to 40%, depending on the SPM level. Also, assumptions about the carbon content of SPM and a constant carbon:chlorophyll ratio are clear oversimplifications.

The last method used to estimate chlorophyll concentration was based on irradiance ratios as described by *Smith et al.* [1991]. Although upwelling radiance is far more sensitive to changes in chlorophyll concentration, downwelling irradiance was used with some success on the Biowatt moorings by *Smith et al.* [1991]. We estimated Chl as

$$\mathrm{Chl} = A\left[\frac{E_d(441)}{E_d(520)}\right]^B \tag{5}$$

$E_d$ is the downwelling irradiance at 441 and 520 nm, and $A$ and $B$ are fitted parameters. *Smith et al.* [1991] report values for $A$ and $B$ at 32, 52, and 72 m depth from the Biowatt mooring. The irradiance method should be much less sensitive to changes in chlorophyll, especially in low-chlorophyll waters. This is expected as downwelling irradiance is integrated over a very short distance. In contrast, the upwelling radiance method used in ocean color remote sensing integrates over one to two optical depths.

Figure 6 shows chlorophyll estimated in 1987 using the strobe fluorescence, Sun-stimulated fluorescence, beam attenuation, and irradiance ratio methods described earlier. We limited the estimates to the period from 2 hours before local solar noon to 2 hours after local solar noon (approximately 1100 to 1500 LT).

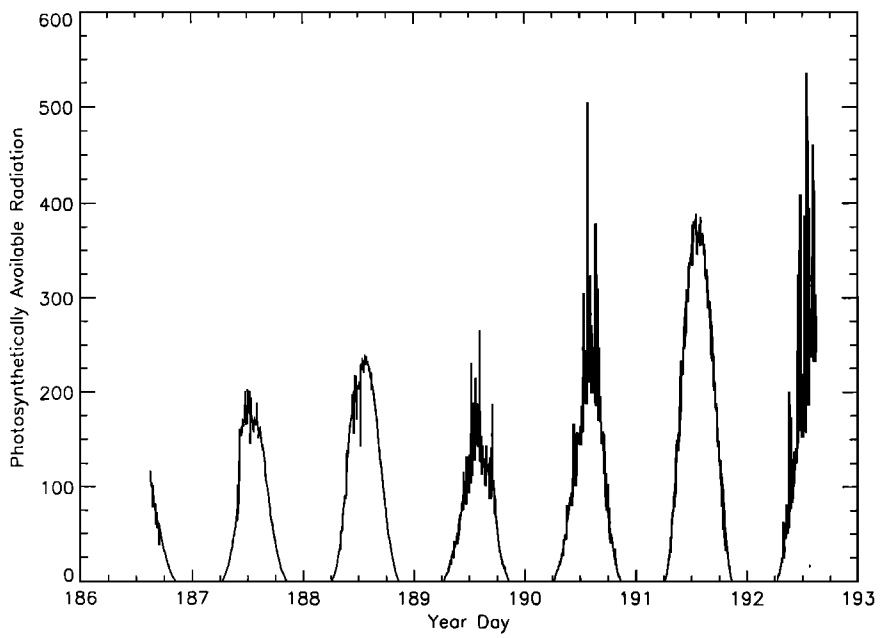


**Figure 3c.** Same as Figure 3a, but for photosynthetically available radiation (in microeinsteins per square meter per second).

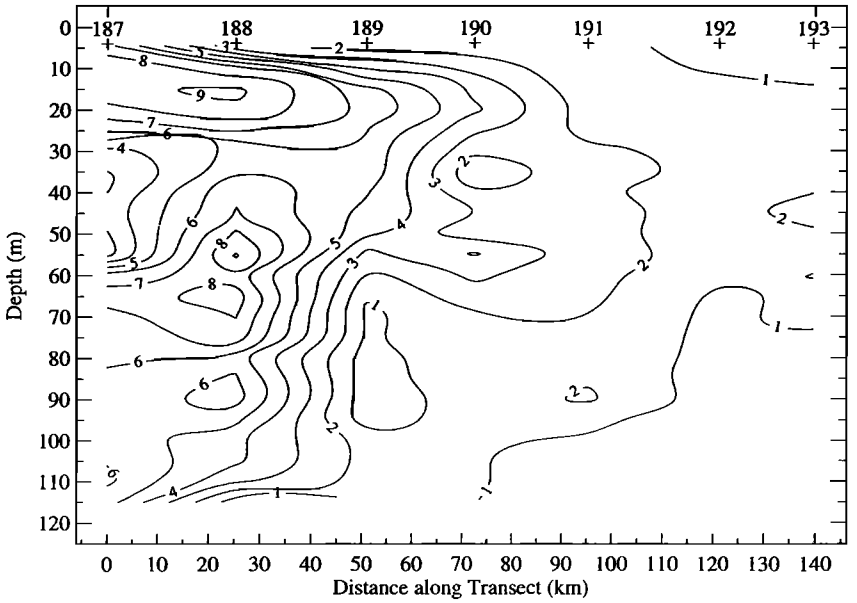


**Figure 4a.** Horizontal section of chlorophyll (milligrams per cubic meter) from vertical profiles collected at approximately noon each day next to the drifter in 1988. Date and location of each profile are marked at the top.

This reduced the effects of changing Sun angle on the observed levels of irradiance. Note that the plots have vertical lines to separate the successive midday periods. The irradiance ratios used the 72-m coefficients estimated by *Smith et al.* [1991]; the coefficients for 35 and 50 m resulted in significantly higher chlorophyll estimates. The Sun-stimulated fluorescence data were converted to chlorophyll using a specific absorption coefficient ($^{o}a_{c}$) of 0.04 and a fluorescence efficiency $\phi_f$ of 0.045 as described by *Kishino et al.* [1984] and *Collins et al.* [1988]. We applied the coefficients described by *Chamberlin et al.* [1990] (0.016 and 0.028 for specific absorption and fluorescence efficiency) and found that the Sun-stimulated fluorescence chlorophyll estimates were consistently higher than the strobe fluorescence estimates by a factor of 3. We therefore relied on the Kishino/Collins parameters for the Sun-stimulated fluorescence model for the 1987 deployment.

Although there are differences in the four chlorophyll estimates, the general patterns of the four time series are similar. This similarity is particularly apparent in the early days of the deployment (days 168–171). The beam attenuation method also predicts much higher pigment values but shows much of the same small-scale structure as the fluorescence methods. Note that the obvious discontinuities that appear in the latter stages of the deployment (days 172–175) are the result of limiting the data to near-noon observations. In particular, the discontinuity between day 172 and day 173 is especially abrupt in the beam attenuation

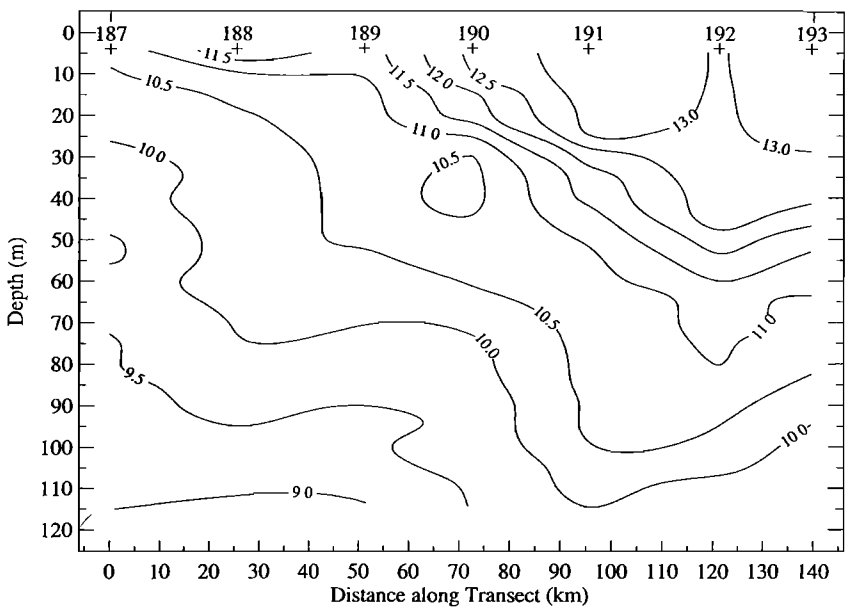


**Figure 4b.** Same as Figure 4a, but for temperature (degrees Celsius).

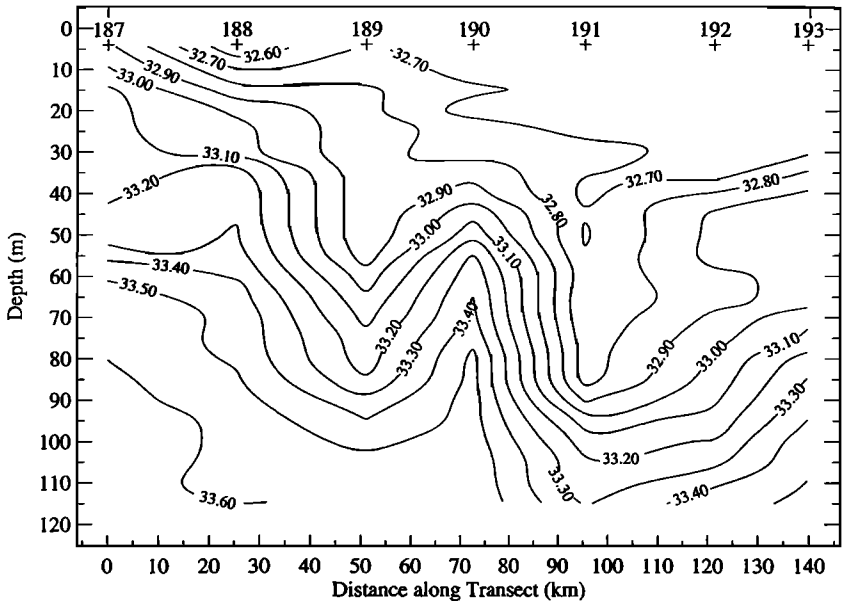


**Figure 4c.** Same as Figure 4a, but for salinity (per mil).

estimate. A similar discontinuity is apparent in the strobe fluorescence method between days 171 and 172.

The two fluorescence methods are surprisingly similar over the duration of the deployment ($r^2$=0.96). Not only do the two fluorescence methods agree on large-scale patterns, but also many of the small-scale features are similar between the two estimates. Given that the strobe fluorescence data were "calibrated" (albeit limited) with chlorophyll extractions, we expect that these estimates are a reasonable measure of the 10-m chlorophyll record along the drifter track. The patterns are quite similar to the chlorophyll map derived by *Hood et al.* [1990] for this region. Relying on both fluorescence-based estimates, chlorophyll concentrations are initially moderate at the beginning of the deployment, increase rapidly, and then decrease precipitously. The high chlorophyll values nearshore from the transmissometer data are likely an artifact of the high particulate, but nonfluorescent, concentrations in the upwelling center [*Abbott et al.*, 1990].

Despite the numerous assumptions in the transmissometer-based chlorophyll estimates (coefficients for converting beam transmission to suspended particulate matter, to carbon, and finally to chlorophyll), the fluorescence methods and the transmissometer method are remarkably similar, differing by a factor of 2 to 3. Although this is a large difference for in situ sampling, the discrepancy is in line with other remote sensing methods such as satellites [*Gordon et al.*, 1983]. Note the monotonic increases on days 173–175. *Abbott et al.* [1990] interpreted this as evidence of daily growth.

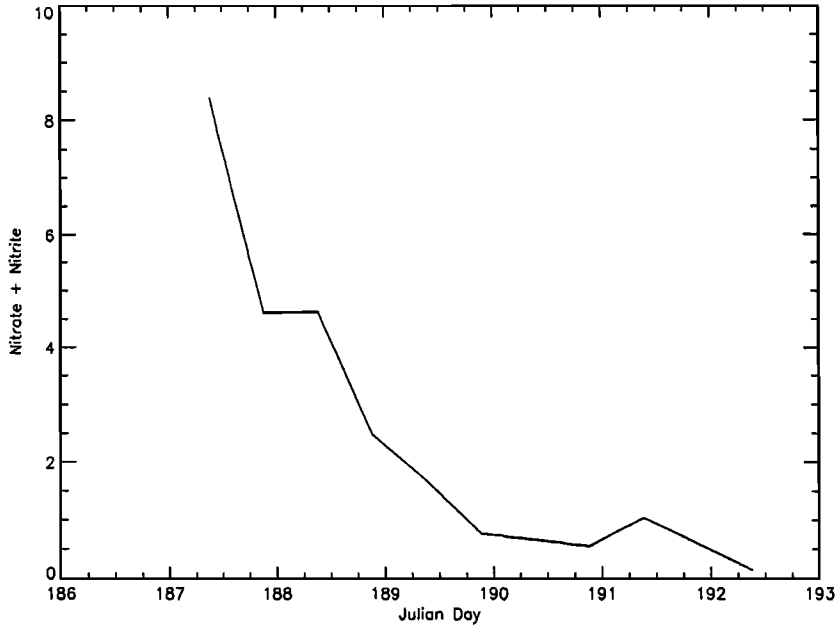


**Figure 5.** Time series of nitrate plus nitrite (N+N) concentrations (micromoles) from the 1988 deployment.

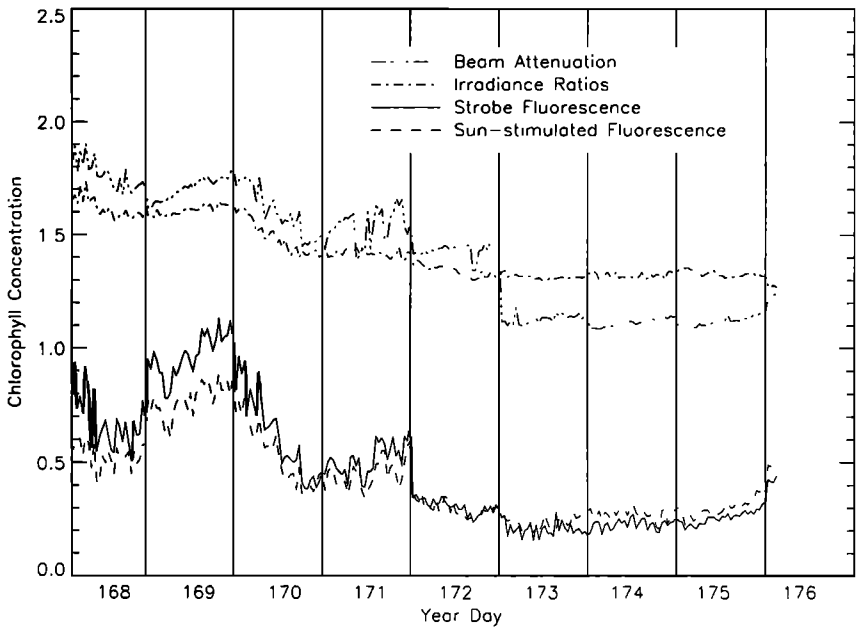


**Figure 6.** Estimates of chlorophyll (milligrams per cubic meter) using four data sets from the 1987 deployment. Observations are constrained to between 1100 and 1500 LT for each day. Vertical lines separate the successive midday periods for each day.

The irradiance method is much less sensitive to changes in concentration, especially at low chlorophyll levels offshore. The general decrease in concentration offshore is consistent with the other estimates, but many small-scale features are not apparent. However, some of the changes in estimated chlorophyll may be the result of physiological changes, especially in the fluorescence-based methods.

The general patterns of chlorophyll were similar in 1988 (Figure 7), although the levels were much higher than in 1987 (Figure 6). The most noticeable difference is between the strobe fluorescence and the Sun-stimulated fluorescence estimates which used the values of specific absorption and fluorescence efficiency presented by *Kishino et al.* [1984] and *Collins et al.* [1988]. These values (0.04, and 0.045, respectively) were used

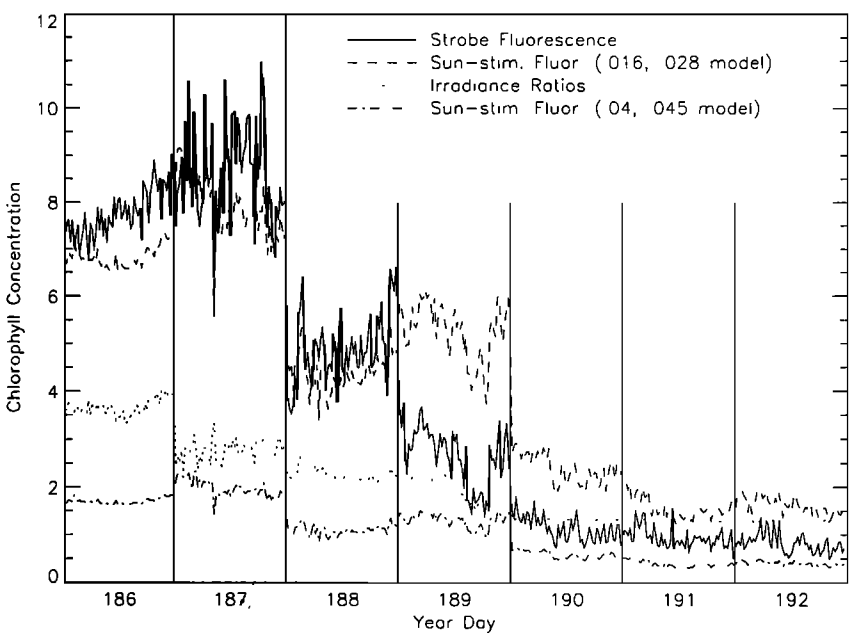


**Figure 7.** Estimates of chlorophyll (milligrams per cubic meter) using three data sets from the 1988 deployment. Observations are constrained to between 1100 and 1500 LT. Vertical lines separate the successive midday periods for each day. The Kishino/Collins parameters (0.04, 0.045 model) [*Kishino et al.*, 1984; *Collins et al.*, 1988] for the Sun-stimulated fluorescence estimates are compared with the Chamberlin parameters (0.016, 0.028 model) [*Chamberlin et al.*, 1990].

for the 1987 deployment. The Sun-stimulated fluorescence estimates of chlorophyll are significantly lower than the calibrated (by daily, in situ sampling next to the drifter) strobe fluorescence estimates by nearly a factor of 3. This difference is especially apparent nearshore in the high chlorophyll waters. We tried different values for the specific absorption coefficient ${}^{o}a_c$ and fluorescence efficiency $\phi_f$ of 0.016 and 0.028, based on *Chamberlin et al.* [1990]. The match between these two fluorescence estimates is much better, especially during the first 3 days of the deployment. After day 188 the Sun-stimulated fluorescence estimates using the Chamberlin coefficients are consistently higher than the strobe fluorescence estimates. Similar variability in these parameters and their effects on estimates of primary productivity from Sun-stimulated fluorescence was observed by *Stegmann et al.* [1992].

These results suggest that there were significant changes in the fluorescence characteristics of the phytoplankton between the 1987 and 1988 deployments. The relationship between the two fluorescence estimates is much more complicated in 1988. First, recall that the strobe fluorescence estimates were calibrated against daily in situ observations; daily changes in this relationship can add variability. The strobe fluorescence calibration coefficient was much smaller on day 189 than at other times, perhaps accounting for at least part of the discrepancy between the two fluorescence methods. Second, changes in the Sun-stimulated fluorescence model parameters are another source of variability. In addition to the apparently large shifts between 1987 and 1988, there appear to be changes in these parameters during the 1988 deployment. It is well known, for example, that fluorescence yield and specific absorption vary as a function of species composition [e.g., *Bricaud et al.*, 1988; *Falkowski and Kiefer*, 1985].

## Estimates of Primary Productivity

We estimated instantaneous primary productivity based on the model described by *Chamberlin et al.* [1990] using Sun-stimulated fluorescence, as modified by *Chamberlin and Marra* [1992] to include a temperature effect. The rate of primary production can be expressed as

$$F_c = \left(\frac{k_{cf}}{k_{cf} + E_o(\mathrm{PAR})}\right) \times \left(\frac{\phi_c}{\phi_f}\right)_{\max} \times (k \times T + c) \times F_f \quad (6)$$

where $k_{cf}$ is the value of the irradiance at 1/2 $(\phi_c/\phi_f)_{\max}$, $(\phi_c/\phi_f)_{\max}$ is the maximum value of the ratio of the quantum yields of photosynthesis and fluorescence. The temperature dependence is modeled as linear function where $T$ is temperature, $k$ is 0.044, and $c$ is 0.257 as determined by *Chamberlin and Marra* [1992]. Using the data described by *Chamberlin et al.* [1990], we assumed that $(\phi_c/\phi_f)_{\max}$ was approximately 2.3 atoms C/photon/einstein (E)/m$^3$/s and that $k_{cf}$ was approximately 133 μE/m$^2$/s (incorrectly stated as mE/m$^2$/s by *Chamberlin et al.* [1990]). After making the necessary unit conversions, we expressed the rate of primary production as nanogram-atoms of Carbon per cubic meter per second, consistent with *Chamberlin et al.* [1990].

In 1987 (Figure 8a), primary productivity was surprisingly uniform along the drifter track, compared with the more intense variability in chlorophyll (Figure 6). It decreased by only a factor of 2 from the beginning to the end of the deployment, whereas chlorophyll decreased by a factor of 4. In comparison, the pattern of productivity was much more variable as the drifter moved offshore in 1988 (Figure 8b), decreasing from 500 to 100 ng-atoms C/m$^3$/s. This variability is largely driven by the variations in chlorophyll, which were also much larger than in 1987 (Figure 7).

The productivity:chlorophyll biomass ratio $P^B$ is shown in Figure 9. Clearly, this ratio was much higher in 1987 than in 1988. Even nearshore, where chlorophyll values were relatively high in both years, phytoplankton were growing more rapidly on a per unit biomass basis in 1987 by a factor of 3 to 5 (Figure 9a).

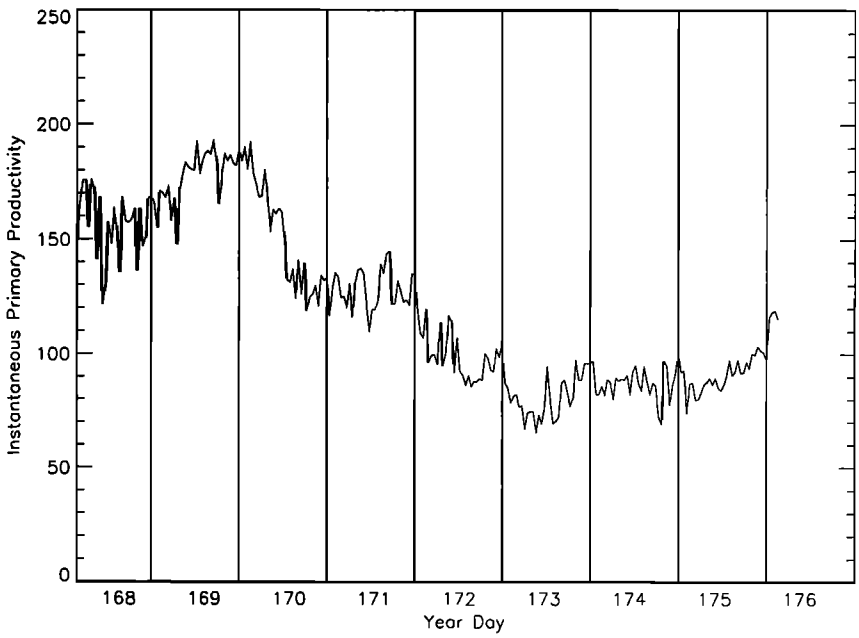


**Figure 8a.** Estimates of instantaneous primary productivity (nanogram atoms of carbon per cubic meter per second) based on Sun-stimulated fluorescence from the 1987 deployment. Observations are constrained to between 1100 and 1500 LT. Vertical lines separate the successive midday periods for each day.

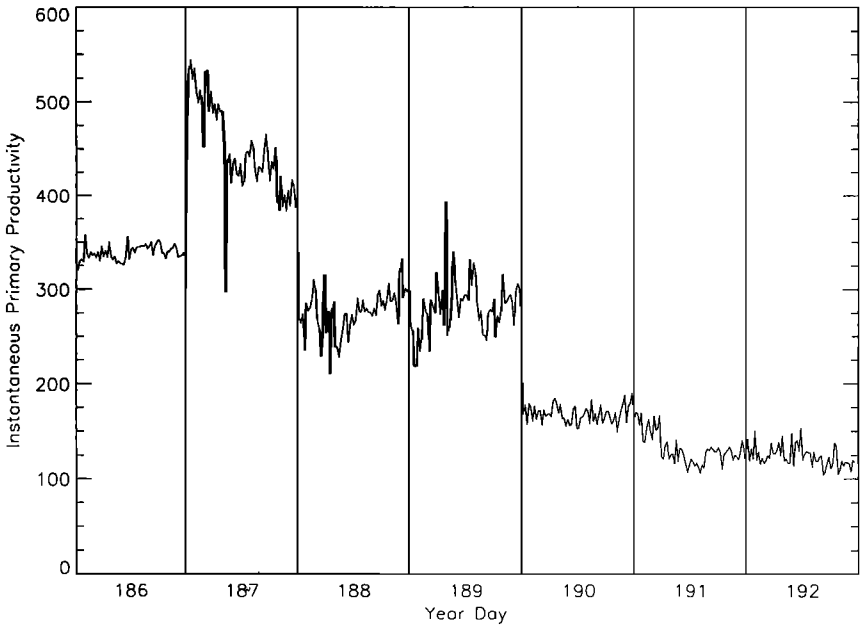


**Figure 8b.** Same as Figure 8a, except from the 1988 deployment.

However, there are numerous assumptions in the productivity and chlorophyll calculations that could cause these estimates to be in error. We compared our $P^B$ estimates in 1987 with those of *Hood et al.* [1991], who used direct $C^{14}$ measurements. Although *Hood et al.* [1991] sampled at somewhat different locations and times in 1987, the range of $P^B$ is about the same, accounting for changes in units. *Chavez et al.* [1991] published maps of chlorophyll and estimates of integrated primary productivity (from a regression model of PAR and chlorophyll) for 1988. While these are not directly comparable to our estimates of near-surface $P^B$, the ratio of integrated productivity to integrated chlorophyll approximately doubled from inshore to offshore, a relative increase similar to that shown in Figure 9b. Thus the patterns of relative changes in $P^B$ are reasonable.

In 1987, $P^B$ was lower on day 169, when chlorophyll was at its highest. $P^B$ was also low on part of day 171 when chlorophyll levels again increased. This suggests that the changes in $P^B$ were dominated by changes in chlorophyll content in 1987. However, the general pattern is for $P^B$ to increase as the drifter moves offshore. In 1988 the pattern is much less variable (in contrast to the productivity and chlorophyll values in Figure 8b and Figure 7). As noted above, the drifter in 1988 more nearly followed the core of the much stronger meander, whereas in 1987 the drifter stayed inshore of the weaker meander. Even offshore, where chlorophyll values were nearly the same in both years, $P^B$ was much higher in 1987. This is consistent with the general pattern of higher absolute productivity in the freshly upwelled water in the core of the meander and lower productivity offshore or in

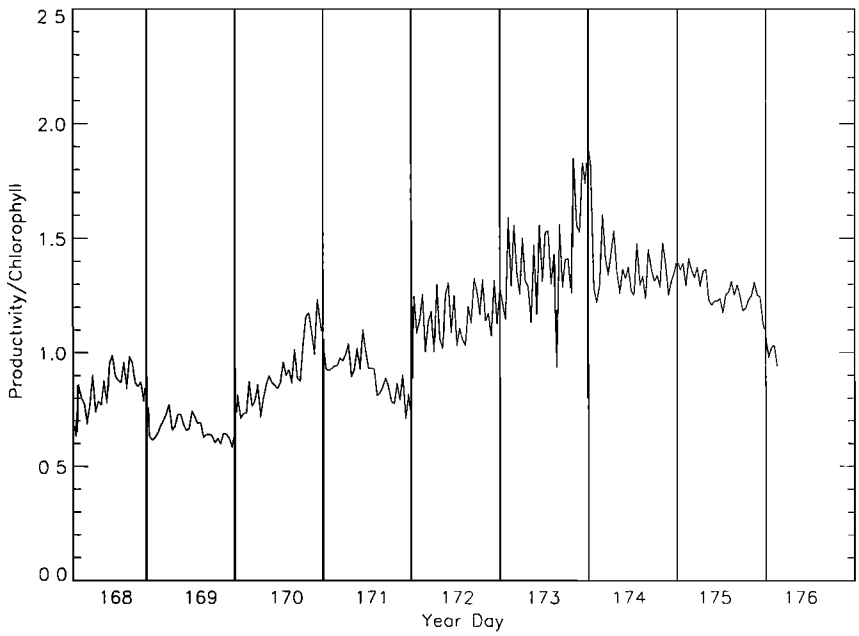


**Figure 9a.** Productivity per unit chlorophyll $P^B$ from the 1987 deployment (in milligrams carbon per milligrams chlorophyll per hour). Vertical lines separate the successive midday periods for each day.

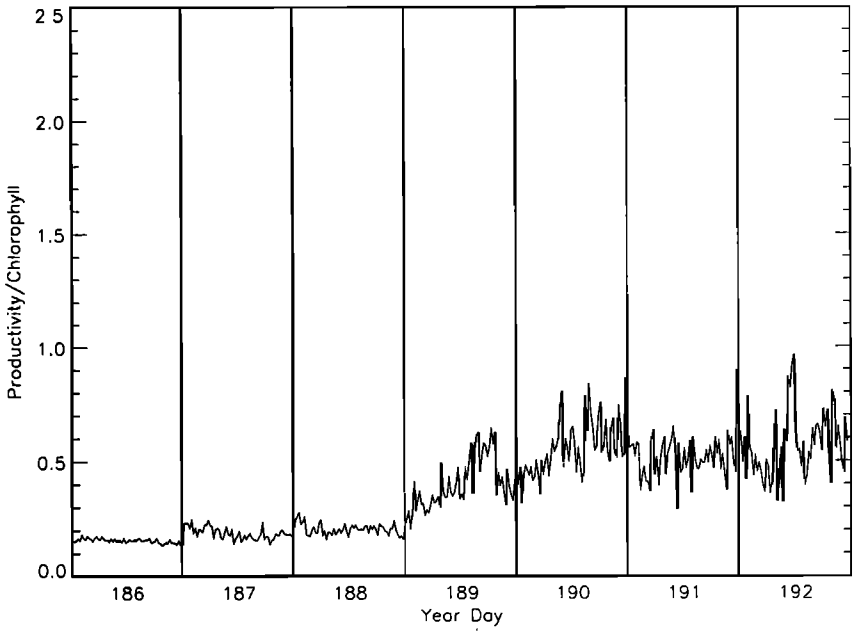


**Figure 9b.** Same as Figure 9a, except from the 1988 deployment.

places or years where the meander is weaker. The patterns of $P^B$, however, are the reverse. A similar pattern was noted by *Hood et al.* [1991]; the highest primary productivity rates were inshore of the meandering jet.

We took all daytime observations (as opposed to a 4-hour window centered around local solar noon) of the flux of Sun-stimulated fluorescence $F_f$ and plotted them versus PAR. This resulted in a family of curves that resembled typical photosynthesis versus irradiance (P-I) curves. We normalized $F_f$ to chlorophyll as estimated from strobe fluorescence. Figures 10a–10d show the relationship between normalized $F_f$ and PAR for both 1987 and 1988. For PAR levels below 200 $\mu E/m^2/s$, the relationships are fairly linear, although the slopes differ between days. The one notable exception is on day 169 in 1987 (Figure 10a); chlorophyll levels were quite variable (Figure 6), and species composition changed considerably [*Abbott et al.*, 1990, Figure 12]. We expect the linear relationship to break down at higher light levels as strobe fluorescence (which was used to estimate chlorophyll) will show some inhibition at high light levels [*Harris*, 1980]. However, the nearly linear relationship still holds even at high PAR levels.

As light is absorbed by phytoplankton, it can be used either in the carbon fixation process, transformed into heat or reemitted as fluorescence [*Falkowski and Kiefer*, 1985]. At low to moderate light levels, there should be nearly linear partitioning between these three processes, which is consistent with these observations.

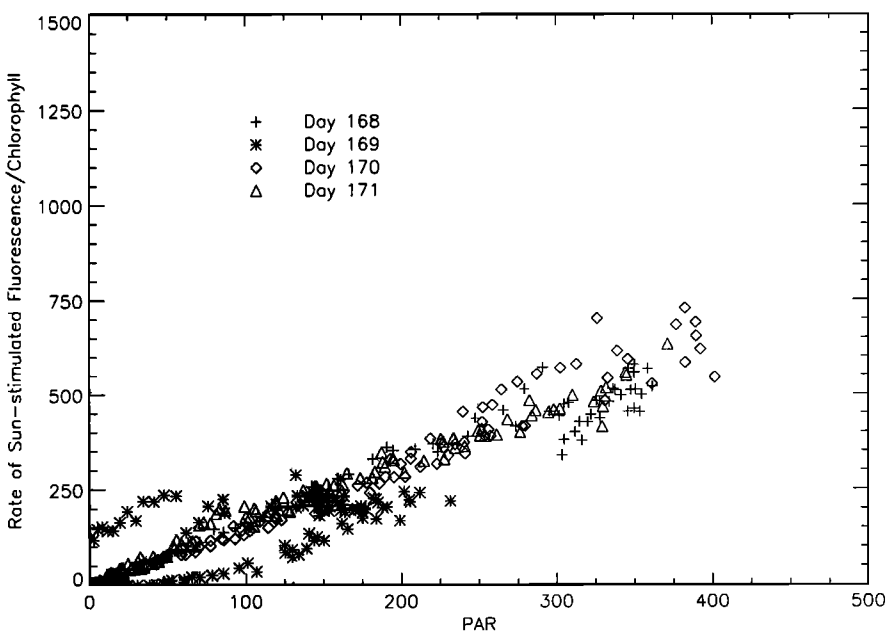


**Figure 10a.** Flux of Sun-stimulated fluorescence per unit chlorophyll (nanoeinsteins per milligram chlorophyll per second) versus photosynthetically available radiation (PAR). Data are shown for inshore regions in 1987.

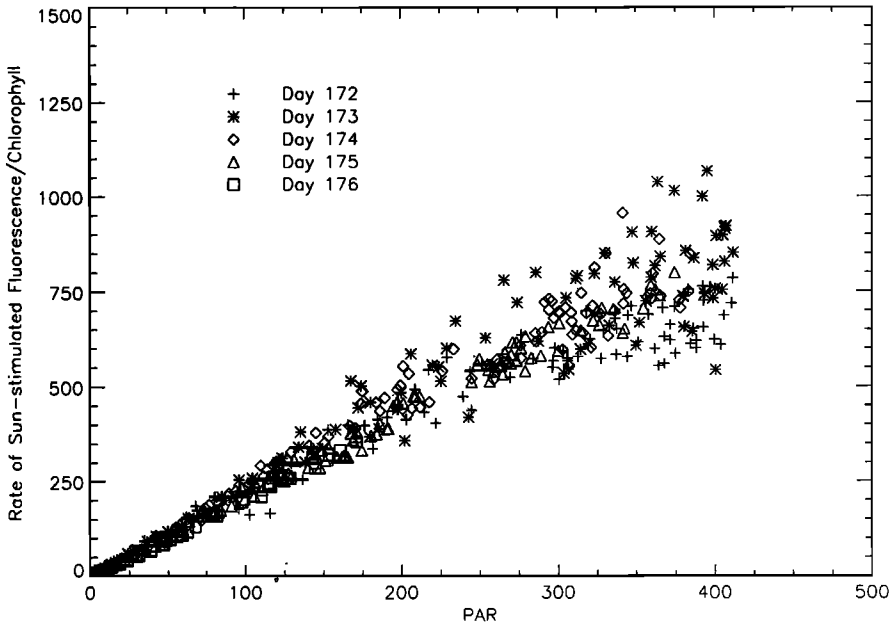


**Figure 10b.** Same as Figure 10a, but for offshore regions in 1987.

However, the partitioning should change, depending on the physiological state of the phytoplankton. As phytoplankton become more nutrient limited, the amount of light reemitted as fluorescence should increase relative to the amount used to fix carbon [*Kiefer and Reynolds*, 1992]. We used linear regression to calculate the slope of the lines for each day except day 169 in 1987 as there appeared to be a much higher level of temporal variability than the other days. These slopes are shown in Table 2. In 1987 the slope increased by 50% as the drifter moved offshore, whereas it more than doubled in 1988. Note that the slopes were much smaller in 1988 than in 1987. Although this is, in essence, just another way of presenting $F_c$ (which is a function of PAR and $F_f$), this result does show the strong change in the partitioning of absorbed light energy and the associated temporal scales. We note that the transition between inshore and offshore properties is more abrupt in 1988 (occurring between day 188 and day 189) than in 1987 when the transition was more gradual. This is consistent with the changes in the strength and width of the meander as seen in the physical measurements of *Kosro et al.* [1991] and *Huyer et al.* [1991].

*Stramska and Dickey* [1992] note that the bio-optical properties of phytoplankton can change rapidly on diel scales, thereby

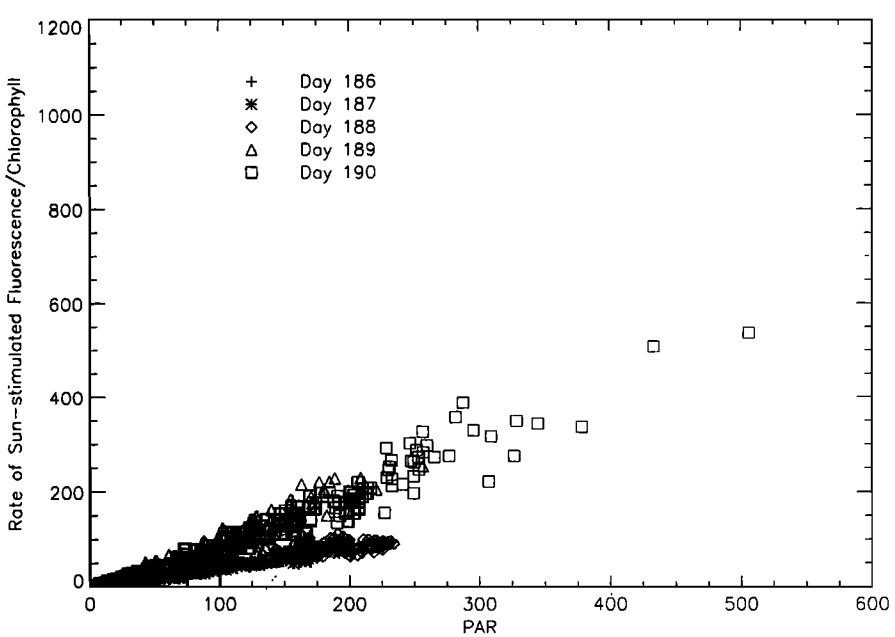


**Figure 10c.** Same as Figure 10a, but for inshore regions in 1988. Note that day 190 has been plotted with both the inshore and offshore regions.

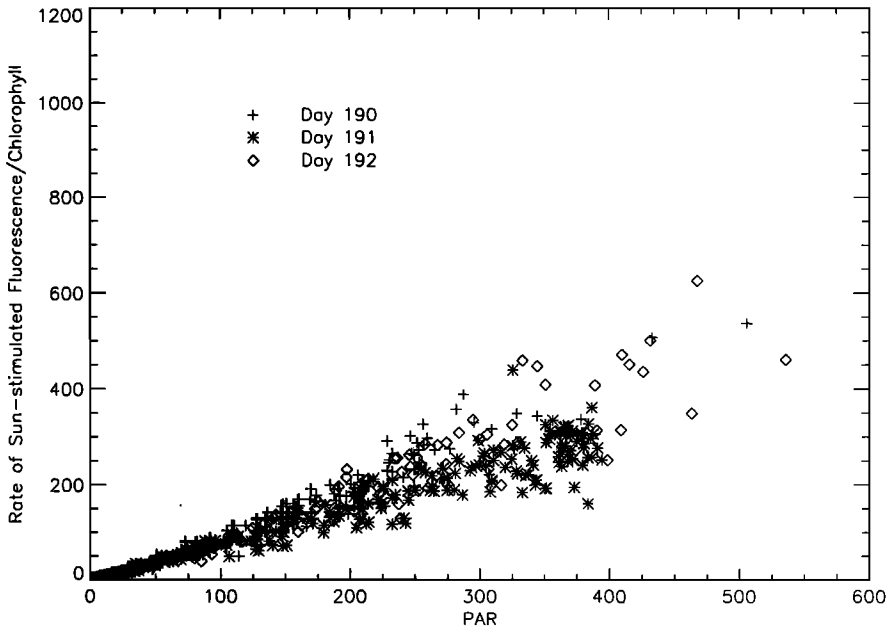


**Figure 10d.** Same as Figure 10a, but for offshore regions in 1988. Note that day 190 has been plotted with both the inshore and offshore regions.

confounding simple interpretation of beam attenuation and fluorescence in terms of either chlorophyll biomass or primary productivity. We thus plotted the ratio of beam attenuation to strobe fluorescence from 1987 as a function of PAR as *Stramska and Dickey* [1992, Figure 17]. Figure 11a shows the nearshore (days 168–171) and Figure 11b, the offshore (days 172–176) data. These are quite similar to the 10-m data from *Stramska and Dickey* [1992], which suggest that much of the diel variation is caused by changes in the bio-optical properties of the phytoplankton. In particular, changes in cellular chlorophyll may change both fluorescence and beam attenuation in parallel during the daylight hours, although processes such as internal waves will complicate this interpretation [*Marra*, 1995]. We note no apparent quenching of fluorescence by PAR, similar to results of *Stramska and Dickey* [1992]. The offset between the inshore waters and the offshore waters implies that there was more scattering and absorption offshore per unit of fluorescence (chlorophyll) as noted by *Abbott et al.* [1990].

**Table 2. Slopes of Linear Regression Between the Rate of Sun-Stimulated Fluorescence (Normalized to Chlorophyll Concentration) and Photosynthetically Available Radiation**

| Day | Slope |
|---|---|
| *1987* | |
| 168 | 1.4 |
| 169 | n/a |
| 170 | 1.7 |
| 171 | 1.5 |
| 172 | 1.7 |
| 173 | 2.1 |
| 174 | 2.1 |
| 175 | 2.1 |
| 176 | 2.1 |
| *1988* | |
| 186 | 0.4 |
| 187 | 0.4 |
| 188 | 0.4 |
| 189 | 1.0 |
| 190 | 1.0 |
| 191 | 0.8 |
| 192 | 1.0 |

### Small-Scale Variability

To examine small-scale patterns, we calculated variance spectra from several of the physical and bio-optical time series. We analyzed only those time series where there was a continuous record (temperature, beam attenuation, and strobe fluorescence). We used maximum entropy methods (MEM) to calculate the spectra; as we limited our discussion to timescales greater than 5 hours, this method should not produce spurious results. Comparison with structure functions showed that the MEM spectra captured the same scales of variability at these longer timescales. We varied the number of poles used to calculate the MEM spectra as well; we used these results to estimate the minimum period that could be reasonably studied based on the robustness of the various spectral peaks. In our case, periods less than 5 hours showed considerable variability in the number of peaks as a function of the number of poles used in the calculation.

To develop error estimates for the spectral estimates, we calculated the MEM spectrum for 10,000 random time series. We used series that had the same number of points as our actual data records and used the same number of poles in the MEM calculations. On the basis of these bootstrap estimates, a factor of 2 around each MEM spectral estimate will fit within plus or minus 2 standard deviations (nearly equivalent to 90% confidence intervals). For example, if the MEM estimate is 10, then the "2 standard deviation" confidence interval extends from 5 to 20.

Figure 12 shows a typical MEM spectrum, in this case beam attenuation from the 1987 record. A strong peak is present with a period of 24 hours, with smaller peaks at 16, 12, 8, and 6 hours. Temperature and especially strobe fluorescence show similar diurnal and semidiurnal peaks. The diurnal signal has been noted

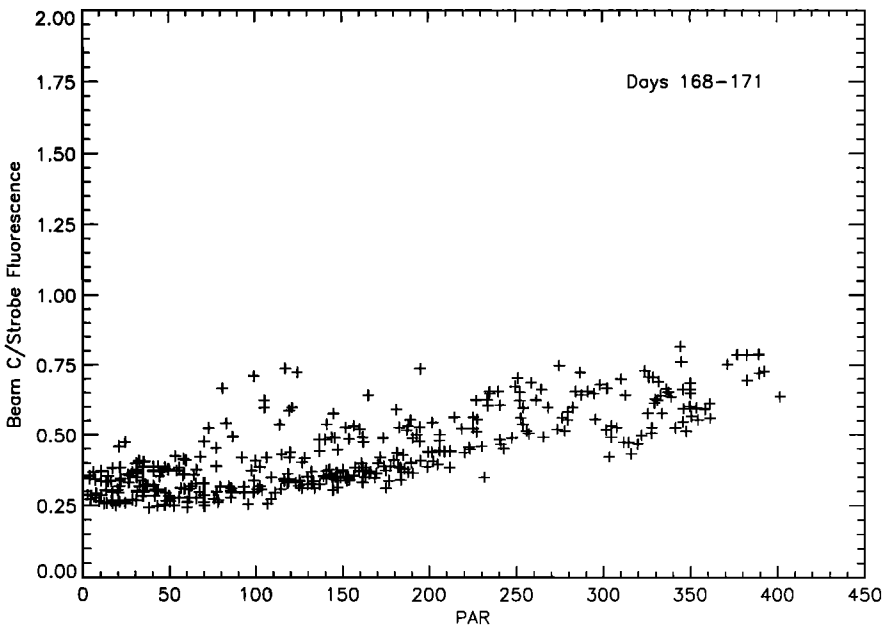


**Figure 11a.** Beam attenuation coefficient versus strobe fluorescence for nearshore regions from the 1987 deployment.

in many other bio-optical records [*Dickey et al.*, 1993; *Stramska and Dickey*, 1992; *Dickey et al.*, 1991]. In the case of strobe fluorescence, diel variability is the result of the changes in fluorescence response to changes in solar irradiance [*Kiefer*, 1973; *Stramska and Dickey*, 1992]. For temperature, diel variability is also the result of changes in solar irradiance which causes near-surface heating during the day and is visible in the offshore portions of the deployments in both years. Beam attenuation is thought to change as a result of both growth in the number of particles as well as changes in their scattering properties [*Ackleson et al.*, 1990]. A peak at the semidiurnal period has not been observed in other bio-optical time series [*Dickey et al.*, 1991] which have strong diurnal signals, but it is quite pronounced in the strobe fluorescence data from the 1987 deployment (Figure 13). Smaller peaks were visible in the temperature and beam attenuation spectra at the semidiurnal period.

A semidiurnal tide may be the cause of this peak, similar to the semidiurnal peaks found in current meter records off northern California [*Noble et al.*, 1987; *Rosenfeld and Beardsley*, 1987]. This could result in water motions which would change the bio-optical and temperature properties of the water at the drifter. Fluorescence could change either as the result of changes in chlorophyll content or as a photoadaptive response to changing light levels as deeper water is brought closer to the surface. Although the strong diurnal signal could result in an overtone to appear at the semidiurnal frequency, note that no such overtone appears in the 1987 fluorescence spectrum (Figure 13).

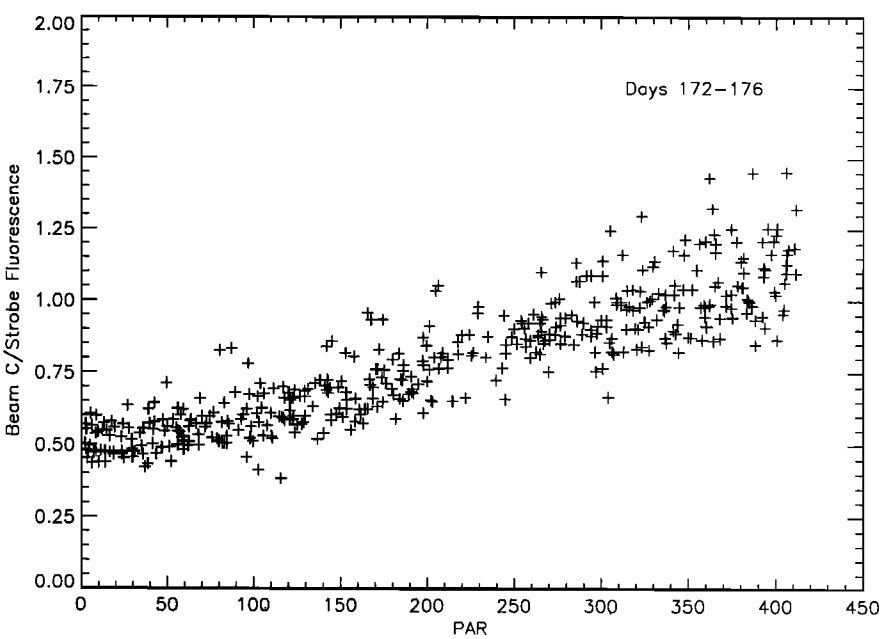


**Figure 11b.** Same as Figure 11a, except for the offshore regions.

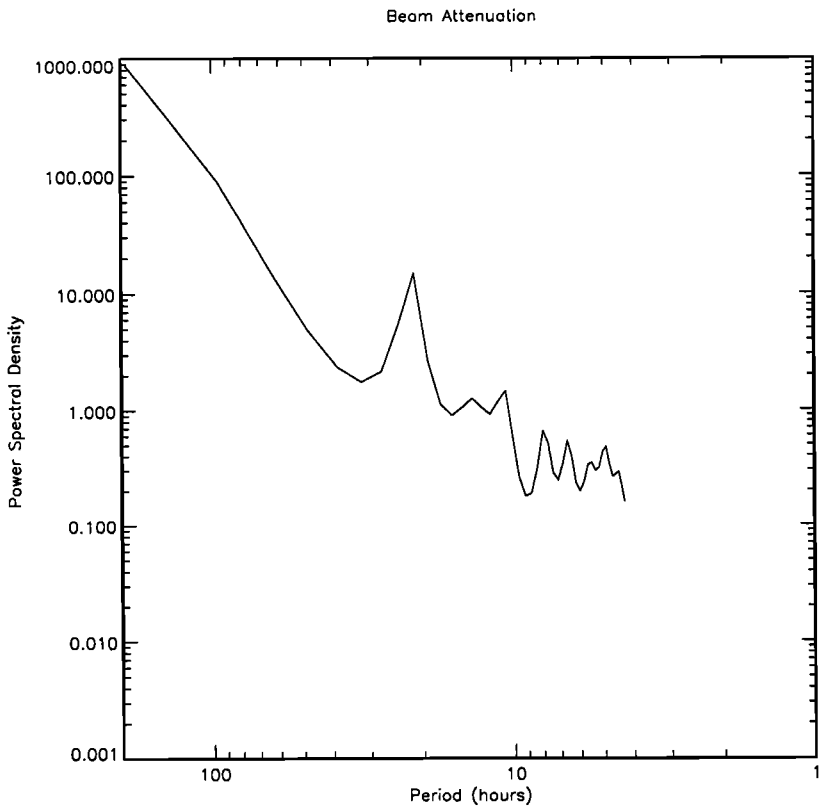


**Figure 12.** Variance spectrum derived using the maximum entropy method for beam attenuation from the 1987 deployment.

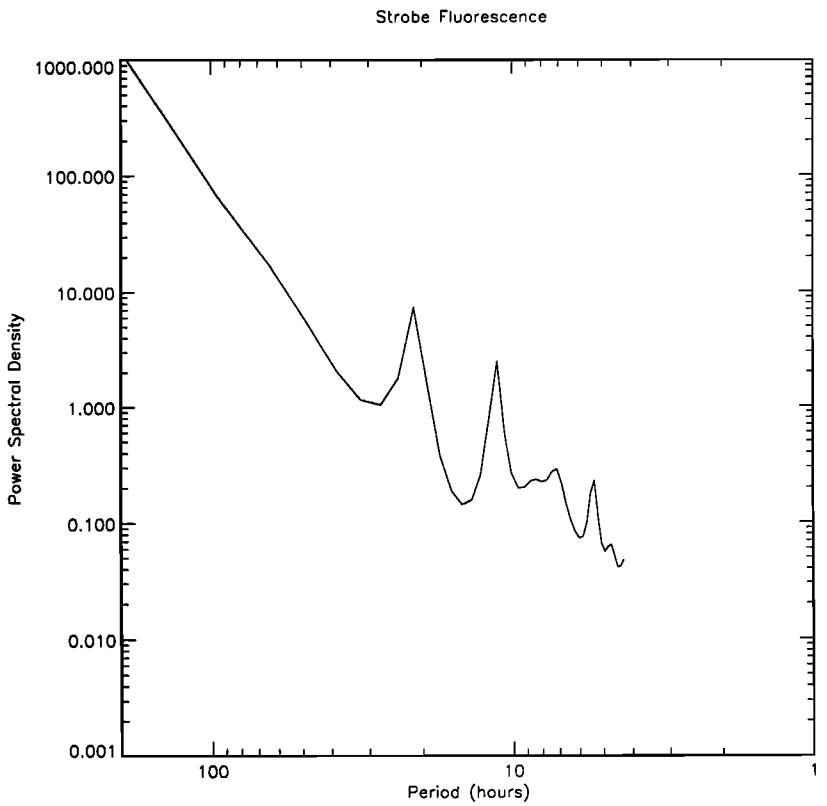


**Figure 13.** Same as Figure 12, except for strobe fluorescence.

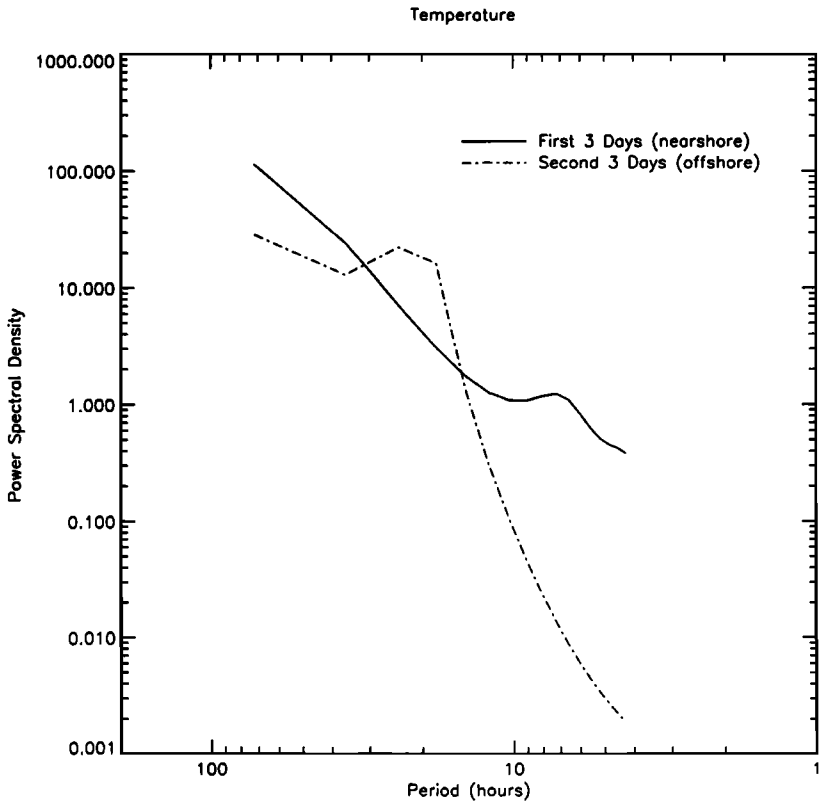


**Figure 14a.** Variance spectrum for temperature from the 1987 deployment. Data were passed through a band reject filter, removing the 24-hour cycle.

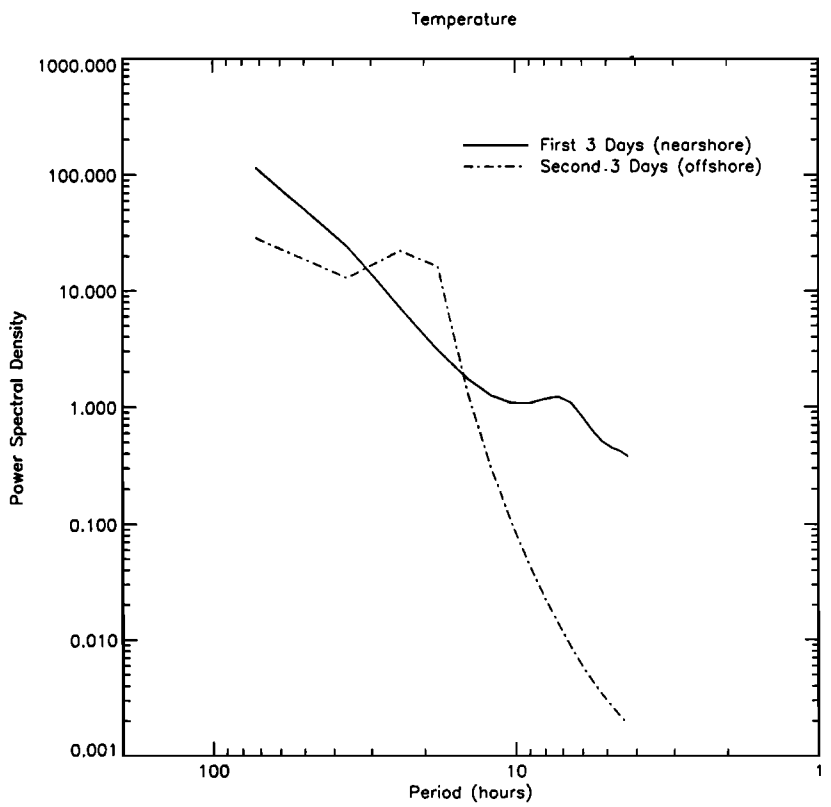


**Figure 14b.** Same as Figure 14a, except from the 1988 deployment.

The patterns of variance appear to differ between nearshore and offshore, so we divided each deployment time series in half. Thus we considered days 168–172 from 1987 and 186–189 from 1988 as the nearshore time series and days 172–176 from 1987 and 189–192 from 1988 as the offshore time series. We passed each time series through a band reject filter, removing the strong diurnal signal from all variables. For strobe fluorescence we removed both the diurnal and semidiurnal signals. Figures 14a and 14b show the MEM spectrum for temperature from both deployments. Although the level of variance is different between the two deployments in the nearshore region, the slopes are nearly identical (about 2). A peak is visible at 10 hours in 1987 (Figure 14a), but in general, neither nearshore spectrum shows much structure. The nearshore spectrum of beam attenuation (Figure 15) is flatter than the nearshore temperature spectrum from 1987 (Figure 14a), with a slope of about 1.5 and a peak at 15 hours rather than at 10 hours. The shapes of the nearshore strobe fluorescence spectra (Figures 16a and 16b) are slightly different, with a slope of 2 in 1987 and 1.5 in 1988. There is a noticeable semidiurnal peak in 1987 (Figure 16a). Despite these subtle differences the nearshore spectra of all three variables are generally similar in their lack of strong peaks. This is most likely a result of the intense, mesoscale variability present in the nearshore region that occurs over a continuum of timescales.

The offshore variance spectra behave much more irregularly. Figure 14 shows the spectra for temperature from the offshore regions in 1987 and 1988. As with the nearshore series, both data sets were passed through a band reject filter to remove the diurnal signal. In 1987 (Figure 14a) the spectrum is dominated by much stronger peaks at 19 and 6 hours than nearshore. In contrast, the 1988 temperature spectrum (Figure 14b) was dominated by a peak near 20 hours. The bio-optical variables also varied in a less continuous manner offshore. Beam attenuation (Figure 15) is dominated by distinct peaks at 48, 20, and 7 hours. Strobe fluorescence (Figure 16) has a peak at 19 hours in both 1987 and 1988, although it is more pronounced in the second year along with a peak at 8 hours in 1988 (Figure 16b) and at 6.5 hours in 1987. Given the lower level of variability in the offshore regions, it is not surprising to see the variance spectra dominated by distinct periods. We have no explanation for the peaks that occur in the 6- to 8-hour range. They may be caused by internal waves which are propagating past the drifter. Of more interest is the consistent peak in the 19–20 hour range.

As the inertial period at this latitude (39°N) is a little over 19 hours, we suspect that the drifter was being subjected to organized inertial motions in the offshore region, similar to those noted by *Paduan and Niiler* [1990] in the CTZ region. These organized motions may have moved the drifter along a front in bio-optical properties as well as temperature. We note that the strength of the inertial peak is much larger in 1988 in both temperature and strobe fluorescence when the drifter was nearly in the core of the meandering jet. As noted by *Paduan and Niiler* [1990] and *Swenson et al.* [1992], the jet is nearly geostrophic in the offshore domain, and there are strong inertial features in the drifter tracks. *Paduan and Niiler* [1990] calculated a horizontal scale of about 3 km for these features. *Swenson et al.* [1992], examining similar scales of motion, estimated vertical motions of 10–20 m/d that were associated with these features. These vertical motions, caused by changes in relative vorticity, are similar to those described for a front in the Sargasso Sea by *Pollard and Regier* [1992]. These strong vertical motions are likely to have a strong effect on the bio-optical properties observed by the drifter package.

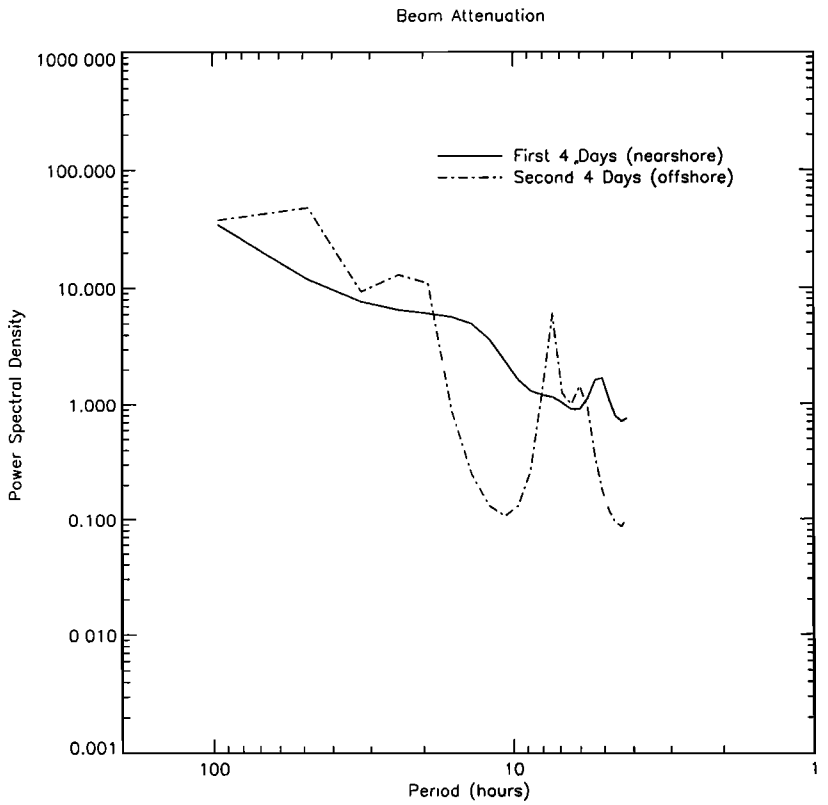


**Figure 15.** Variance spectrum for beam attenuation from the 1987 deployment. Data were passed through a band reject filter, removing the 24-hour cycle.

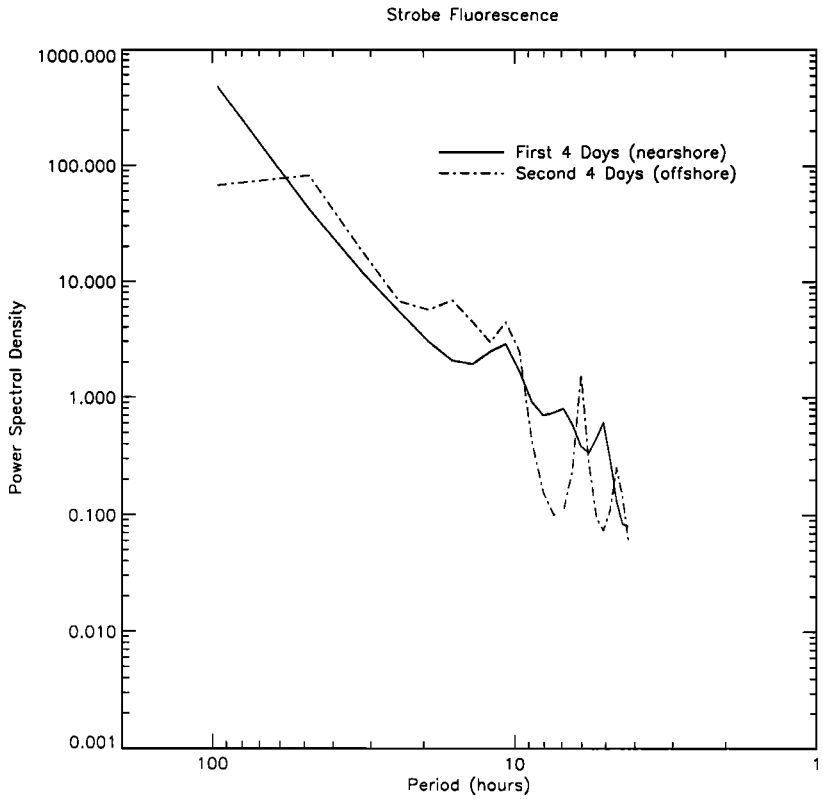


**Figure 16a.** Variance spectrum for strobe fluorescence from the 1987 deployment. Data were passed through a band reject filter, removing the 12- and 24-hour cycles.

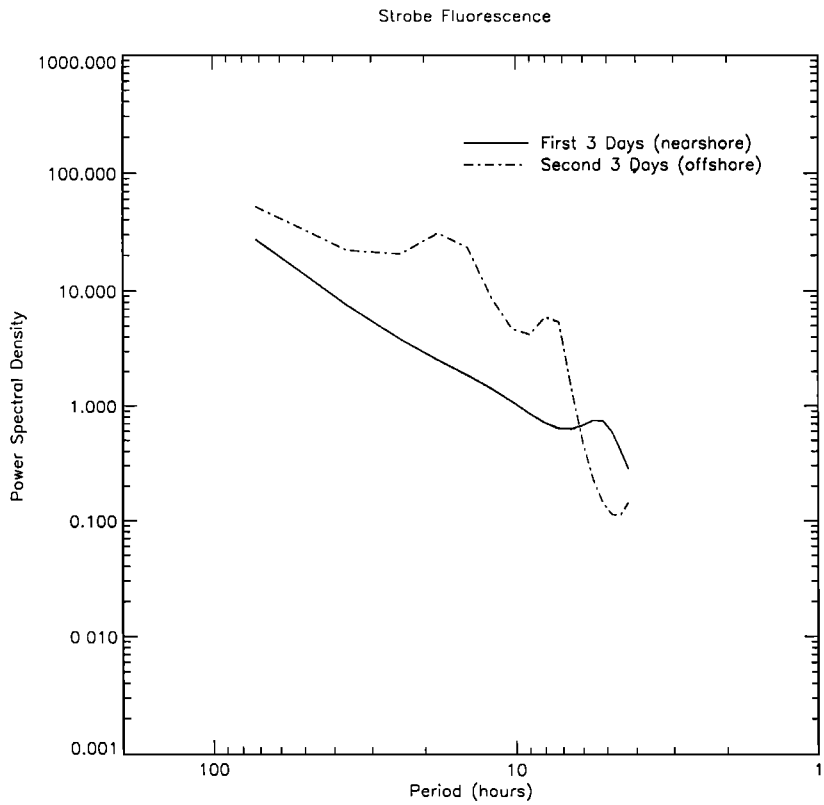


**Figure 16b.** Same as Figure 16a, except from the 1988 deployment.

We tested the performance of our band reject filter with time series composed of sinusoid functions contaminated by random noise. The filter successfully removed the desired frequencies, so we do not think that the 19- to 20-hour peak is an artifact caused by the removal of the 24-hour signal.

## 4. Discussion

While we expect that bio-optical parameters should change from one oceanic domain to another, these observations show that they vary on much smaller scales than might be expected. The interplay between physical forcing and physiological response of the phytoplankton will complicate the application and interpretation of bio-optical algorithms. However, this variability may also be used to understand the processes of response and adaptation, if the appropriate ancillary data are collected.

One such ancillary data set will be information on phytoplankton species composition. Figure 17 shows the 1988 species composition as a percentage of total cell volume. During the first 3 days of the deployment the phytoplankton community was dominated by *Chaetoceros spp.* and other centric diatoms. On day 189 the composition changed dramatically, with *Rhizosolenia* replacing *Chaetoceros*. The final shift was to a community dominated by dinoflagellates. Although a similar replacement of *Chaetoceros* by *Rhizosolenia* occurred in 1987 [*Abbott et al.*, 1990], the magnitude of the shift was not as dramatic. In 1987 the shift was from 35% *Chaetoceros* to 30% *Rhizosolenia*, whereas the shift in 1988 was from 55% *Chaetoceros* to 45% *Rhizosolenia*. In 1987 the community was dominated by large centric diatoms in the offshore waters compared with dinoflagellates in 1988. Given the increased variability in species composition in 1988, it is not surprising to see large differences in the fluorescence response.

Changes in the physical environment are likely the ultimate cause of the species changes. Figure 3 shows the temperature changes along the drifter path. Before day 190, temperatures are cool and variable. The temperature increases sharply by 2°C in 12 hours at day 190, and this front is associated with the shift to dinoflagellates (Figure 17). However, nutrients decrease rapidly before the temperature front is reached. *Swenson et al.* [1992] used two methods to estimate vertical velocities, based on estimates of the heat budget and the vorticity budget. Although there were significant differences in the magnitude of the velocity estimates, the general patterns of upwelling and downwelling were quite similar. The larger estimates from the heat budget approach ranged from 70 m/d downwelling to 40 m/d upwelling, whereas the vorticity estimates were about a factor of 3 smaller. However, as noted by *Swenson et al.* [1992], the heat budget estimates were based on a subcluster of drifters and represented a region of about 60 $km^2$ compared with 150 $km^2$ for the vorticity budget estimates. Initially, the bio-optical drifter was in a region of downwelling (about 40 m/d, based on the heat budget estimates) nearshore. This changed to moderate upwelling (about 20 m/d) on day 188. The drifter then experienced moderate downwelling about midway through day 188. Strong downwelling occurred during day 189 at the same time that *Chaetoceros* was replaced by *Rhizosolenia*. This downwelling was associated with an "instability" identified by *Swenson et al.* [1992] and a westward turn of the drifter. Note the strong front at 70 km (Figure 4a). As *Rhizosolenia* are generally buoyant, their increase on day 189 in association with this front is not unexpected. This was followed by weak upwelling on days 190 and 191 as dinoflagellates came to dominate the phytoplankton. We noted earlier that the normalized rate of Sun-stimulated fluorescence changed dramatically on day 189 (Table 2). This change in physiological response is consistent with the change in physical forcing and species composition.

Given the complex flow patterns in this region, it is not surprising to see strong interleaving of various water masses characterized by different phytoplankton communities. Following

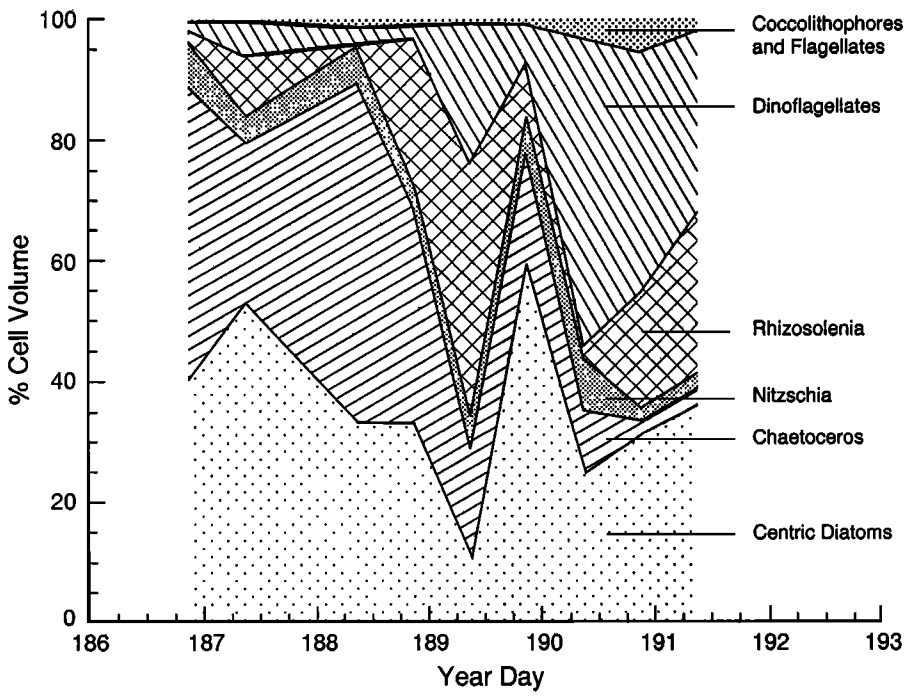


**Figure 17.** Relative phytoplankton species abundance from the 1988 deployment in terms of percent total cell volume.

the description laid out by *Strub et al.* [1991], we define the broad, cold, productive regions as the filaments which are separated from the warmer, less productive offshore waters by a meandering jet. As the drifter does not exactly follow a single water parcel, it may traverse these various water types. It is apparent from these data that the physical dynamics of the coastal transition zone affect the timing and nature of the species changes as observed by the drifter.

A general picture emerges from the two drifter deployments. Changes in the strength of the meander correspond with changes in species composition, primary productivity, and $P^B$. Biomass and primary productivity decrease offshore as nutrients become depleted, but $P^B$ increases. Phytoplankton become more strongly scattering per unit chlorophyll in offshore waters. Thus the meander represents a sharp demarcation between both the biological and bio-optical properties of the phytoplankton. Physical processes such as upwelling and downwelling along the meander play an important role in the smaller-scale variability of these properties. In 1987, when the drifter was somewhat inshore of the main meander, these properties tended to change more gradually over the course of the deployment. In contrast, the deployment in 1988 more nearly followed the core of the meander, and the bio-optical properties changed more abruptly over time. This resulted in more abrupt changes in the biological/physical regime as observed in 1988 and more intense inertial motions.

The presence of intense vertical motions along the drifter path, either through subduction processes [*Kadko et al.*, 1991; *Washburn et al.*, 1991] or through vorticity adjustments caused by inertial motions, obviously complicates the interpretation of the drifter data. As noted earlier, phytoplankton species composition changes considerably in association with changes in the direction of vertical motion. However, we are able to interpret the patterns of temporal change in terms of changes in the physical circulation field. While we cannot assume that the drifter is truly following a patch of phytoplankton, these data show the influence of inertial and tidal motions on bio-optical properties as well as the larger-scale changes that occur between nearshore and offshore or between years.

## 5. Summary and Conclusions

The two deployments of a bio-optical drifter in the coastal transition zone off northern California were analyzed in terms of the performance of several bio-optical algorithms and in terms of large- and small-scale variability. With the availability of long-term bio-optical sampling we need to understand the limits and advantages of these data sets. Bio-optical relationships can change dramatically on a wide range of time and length scales, thus complicating any analysis.

The general features of the waters off northern California were similar in the 2 years. Chlorophyll, particulate concentration, and primary productivity were higher and more variable in the nearshore waters than offshore. $P^B$ and scattering per unit chlorophyll, however, were lower nearshore and higher offshore. The separation between nearshore and offshore properties was delineated by the meandering jet, which separated distinct phytoplankton communities, based on species counts. Similar distinctions were noted by *Hood et al.* [1991] and *Chavez et al.* [1991] for the coastal transition zone region. There were significant changes in species composition (and size structure of the community), both along the drifter tracks and between the two deployments. Although the phytoplankton sampling ceased to operate in the far offshore waters, other observations showed that this region was dominated by small forms, primarily flagellates [*Hood et al.*, 1991].

We applied several methods to estimate chlorophyll using downwelling irradiance ratios [*Smith et al.*, 1991], beam attenuation [*Siegel et al.*, 1989], Sun-stimulated fluorescence [*Chamberlin et al.*, 1990], and conventional strobe fluorescence. Although the general patterns were similar (high, variable chlorophyll values nearshore, decreasing rapidly as the drifter moved offshore), there was considerable difference in the detailed structure of the time series. The relationship between chlorophyll derived from strobe fluorescence and that derived from Sun-stimulated fluorescence differed considerably between 1987 and 1988. In the latter deployment a different set of coefficients for Sun-stimulated fluorescence was required to obtain agreement between the two fluorescence estimates, and these coefficients needed to be altered along the drifter track as it moved from nearshore to offshore. It appeared that strong changes in the phytoplankton community were largely responsible for the changes in the fluorescence relationships. The beam attenuation data were available only during the first deployment, but they revealed strong onshore/offshore differences in bio-optical properties, especially in the amount of scattering per unit chlorophyll.

We examined small-scale variability through variance spectral analysis. A strong diel signal was present in many of the bio-optical variables, as expected. In particular, strobe fluorescence showed a consistent pattern in relation to the amount of solar radiation. Beam attenuation showed a similar diel pattern in the offshore waters. We suggest that this is the result of grazing activity, but changes in the optical properties of phytoplankton would cause a similar pattern. A semidiurnal signal was present in temperature and strobe fluorescence and is perhaps related to the semidiurnal tide. An unexpected peak was found at the inertial period (19 hours) in the bio-optical variables and in temperature. This peak, however, was present only in the offshore waters in both 1987 and 1988. Organized inertial motions of the drifter in the offshore portion of the meander have been observed in other drifter data sets from northern California. These inertial motions are sometimes associated with strong vertical motions caused by changes in relative vorticity. The bio-optical properties varied in response either to these vertical motions or to changes in the relative horizontal position of the drifter as it moved along the meander.

The proximate cause for the temporal and spatial fluctuations in bio-optical properties was changes in the physiological response of the phytoplankton community which was driven by variability in phytoplankton species composition. Such species dependence has been noted in many studies and is not unexpected. The ultimate cause, however, appears to be changes in the physical environment. For example, the strength of the meander as well as distance from the meander appeared to affect the phytoplankton species composition as noted also by *Chavez et al.* [1991]. Similarly, vertical velocities associated with organized inertial motions in the offshore region result in a pronounced bio-optical response.

Similar concerns were raised about fluorometric methods when they were introduced nearly 30 years ago. Many of the problems were addressed simply by more frequent calibration samples. However, it is clear that such calibration sampling must be done on a scale appropriate for the inherent variability in the process under study. Unfortunately, we know little about these scales in the bio-optical realm. Of more concern is the recent availability of unattended sampling devices where calibration

sampling is not possible. Analysis of such data must be conducted with the awareness that variability in the relationships of interest (such as beam attenuation and particulate abundance) will have its own temporal and spatial scales. Thus studies of biological variability must also focus on the variability in the processes used to convert the sensor data (beam transmission, fluorescence, absorption, etc.) into the biological data of interest (particulate concentration, chlorophyll content, etc.).

We are beginning to collect information on the temporal and spatial scales of variability that will be useful in future data assimilation models. While we cannot hope to measure all processes on all relevant scales, more systematic observations of such temporal and spatial variability must be undertaken. Future work must extend these observations over a broad range of physical and biological conditions as it is apparent that the scales of variability can change dramatically, depending on the physical environment.

**Acknowledgments.** We thank P. Niiler for providing the drifters and assisting with design and deployment. We thank R. Hood for design and construction of the drifter packages for the second deployment. G. Friederich provided technical assistance for the water sampler. R. Limeburner and T. Cowles assisted with deployments. Useful discussions were held with R. Letelier, and valuable comments were provided by J. Marra and an anonymous reviewer. B. Barksdale assisted with programming and data analysis. This work was supported by the Office of Naval Research (grants to M.R.A and K.H.B.) and by the National Aeronautics and Space Administration (grants to M.R.A. and C.O.D).

## References

Abbott, M. R., Phytoplankton patchiness: Ecological implications and observation methods, in *Patch Dynamics*, edited by S. A. Levin, T. M. Powell, and J. H. Steele, pp. 37 49, Springer-Verlag, New York, 1993.

Abbott, M. R., K. H. Brink, C. R. Booth, D. Blasco, L. A. Codispoti, P. P. Niiler, and S. R. Ramp, Observations of phytoplankton and nutrients from a Lagrangian drifter off northern California, *J. Geophys. Res.*, *95*, 9393–9409, 1990.

Ackleson, S. G., J. J. Cullen, J. Brown, and M. P. Lesser, Some changes in the optical properties of marine phytoplankton in response to high light intensity, Ocean Optics 10, *Proc. SPIE Int. Soc. Opt. Eng.*, *1302*, 238–249, 1990.

Bartz, R., R. V. Zaneveld, and H. Pak, A transmissometer for profiling and moored observations in water, *Proc. Soc. Photo. Opt. Instrum. Eng.*, *160*, 102–108, 1978.

Bishop, J. K. B., The correction and suspended material calibration of Sea Tech transmissometer data, *Deep Sea Res.*, *Part A*, *33*, 121–134, 1986.

Bricaud, A., A.-L. Bedhomme, and A. Morel, Optical properties of diverse phytoplanktonic species: Experimental results and theoretical interpretation, *J. Plankton Res.*, *10*, 851–873, 1988.

Brink, K. H., and T. J. Cowles, The coastal transition zone program, *J. Geophys. Res.*, *96*, 14,637–4,647, 1991.

Brink, K. H., R. C. Beardsley, P. P. Niiler, M. Abbott, A. Huyer, S. Ramp, T. Stanton, and D. Stuart, Statistical properties of near-surface flow in the California coastal transition zone, *J. Geophys. Res.*, *96*, 14,693–14,706, 1991.

Bryan, F., Parameter sensitivity of primitive equation ocean general circulation models, *J. Phys. Oceanogr.*, *17*, 970–985, 1987.

Chamberlin, S., and J. Marra, Estimation of photosynthetic rate from measurements of natural fluorescence: Analysis of the effects of light and temperature, *Deep Sea Res., Part I*, *39*, 1695–1706, 1992.

Chamberlin, W. S., C. R. Booth, D. A. Kiefer, J. H. Morrow, and R. C. Murphy, Evidence for a simple relationship between natural fluorescence, photosynthesis, and chlorophyll in the sea, *Deep Sea Res., Part I*, *37*, 951–973, 1990.

Chavez, F. P., R. T. Barber, P. M. Kosro, A. Huyer, S. R. Ramp, T. P. Stanton, and B. Rojas de Mendiola, Horizontal transport and the distribution of nutrients in the coastal transition zone off northern California: Effects on primary production, phytoplankton biomass, and species composition, *J. Geophys. Res.*, *96*, 14,833–14,848, 1991.

Chelton, D. B., and M. G. Schlax, Estimation of time averages from irregularly spaced observations: With application to coastal zone color scanner estimates of chlorophyll concentration, *J. Geophys. Res.*, *96*, 14,669–14,692, 1991.

Collins, D. J., C. R. Booth, C. O. Davis, D. A. Kiefer, and C. Stallings, A model of the photosynthetically available and usable irradiance in the sea, Ocean Optics 9, *Proc. SPIE Int. Soc. Opt. Eng.*, *925*, 87–100, 1988.

Denman, K. L., and H. J. Freeland, Correlation scales, objective mapping and a statistical test of geostrophy over the continental shelf, *J. Mar. Res.*, *43*, 517–539, 1985.

Denman, K. L., and T. M. Powell, Effects of physical processes on planktonic ecosystems in the coastal ocean, *Oceanogr. Mar. Biol.*, *22*, 125–168, 1984.

Dickey, T. D., The emergence of concurrent high-resolution physical and bio-optical measurements in the upper ocean and their applications, *Rev. Geophys.*, *29*, 383–413, 1991.

Dickey, T. D., J. Marra, T. Granata, C. Langdon, M. Hamilton, J. Wiggert, D. Siegel, and A. Bratkovich, Concurrent high resolution bio-optical and physical time series observations in the Sargasso Sea during the spring of 1987, *J. Geophys. Res.*, *96*, 8643–8663, 1991.

Dickey, T. D., et al., Seasonal variability of bio-optical and physical properties in the Sargasso Sea, *J. Geophys. Res.*, *98*, 865–898, 1993.

Falkowski, P., and D. A. Kiefer, Chlorophyll *a* fluorescence in phytoplankton: Relationship to photosynthesis and biomass, *J. Plankton Res.*, *7*, 715–731, 1985.

Friederich, G. E., P. J. Kelly, and L. A. Codispoti, An inexpensive moored water sampler for investigating chemical variability, in *Tidal Mixing and Plankton Dynamics*, edited by M. J. Bowman, C. M. Yentsch, and W. T. Peterson, pp. 463–482, Springer-Verlag, New York, 1986.

Gordon, H. R., D. K. Clark, J. W. Brown, O. B. Brown, R. H. Evans, and W. W. Broenkow, Phytoplankton pigment concentrations in the Middle Atlantic Bight: Comparison between ship determinations and coastal zone color scanner estimates, *Appl. Optics*, *22*, 20–36, 1983.

Gordon, H. R., O. B. Brown, R. H. Evans, J. W. Brown, R. C. Smith, K. S. Baker, and D. K. Clark, A semianalytic radiance model of ocean color, *J. Geophys. Res.*, *93*, 10,909–10,924, 1988.

Harris, G. P., The relationship between chlorophyll *a* fluorescence, diffuse attenuation changes and photosynthesis in natural phytoplankton populations, *J. Plankton Res.*, *2*, 109–127, 1980.

Harris, G. P., Phytoplankton Ecology: Structure, Function, and Fluctuation, 384 pp., Chapman and Hall, London, 1986.

Hood, R., M. R. Abbott, P. M. Kosro, and A. Huyer, Relationships between physical structure and biological pattern in the surface layer of a northern California upwelling system, *J. Geophys. Res.*, *95*, 18,081–18,094, 1990.

Hood, R., M. R. Abbott, and A. E. Huyer, Phytoplankton and photosynthetic light response in the coastal transition zone off northern California in June 1987, *J. Geophys. Res.*, *96*, 14,769–14,780, 1991.

Huyer, A., P. M. Kosro, J. Fleischbein, S. R. Ramp, T. Stanton, L. Washburn, F. P. Chavez, T. J. Cowles, S. D. Pierce, and R. L. Smith, Currents and water masses of the coastal transition zone off northern California, June to August 1988, *J. Geophys. Res.*, *96*, 14,809–14,831, 1991.

Kadko, D. C., L. Washburn, and B. Jones, Evidence of subduction within cold filaments of the northern California coastal transition zone, *J. Geophys. Res.*, *96*, 14,909–14,926, 1991.

Kiefer, D. A., Chlorophyll *a* fluorescence in marine centric diatoms: Responses of chloroplasts to light and nutrients, *Mar. Biol.*, *23*, 39–46, 1973.

Kiefer, D. A., and R. A. Reynolds, Advances in understanding phytoplankton fluorescence and photosynthesis, in *Primary Productivity and Biogeochemical Cycles in the Sea*, edited by P. G. Falkowski and A. D. Woodhead, pp. 155–174, Plenum, New York, 1992.

Kiefer, D. A., W. S. Chamberlin, and C. R. Booth, Natural fluorescence of chlorophyll *a*: Relationship to photosynthesis and chlorophyll concentration in the western South Pacific gyre, *Limnol. Oceanogr.*, *34*, 868–881, 1989.

Kishino, M., S. Sugihara, and N. Okami, Estimation of quantum yield of chlorophyll *a* fluorescence from the upward irradiance spectrum in the sea, *La Mer*, *22*, 233–240, 1984.

Kosro, P. M., et al., The structure of the transition zone between coastal waters and the open ocean off northern California, winter and spring 1987, *J. Geophys. Res.*, *96*, 14,707–14,730, 1991.

Marra, J., Capabilities and merits of long-term bio-optical moorings, in *Optical Oceanography*, edited by R. Spinrad and M. J. Perry, Cambridge University Press, New York, 1995.

Niiler, P. P., R. E. Davis, and H. J. White, Water-following characteristics of a mixed layer drifter, *Deep Sea Res., Part A, 34*, 1867–1881, 1987.

Noble, M., L. K. Rosenfeld, R. L. Smith, J. V. Gardner, and R. C. Beardsley, Tidal currents seaward of the northern California continental shelf, *J. Geophys. Res., 92*, 1733–1744, 1987.

Paduan, J. D., and P. P. Niiler, A Lagrangian description of motion in northern California coastal transition filaments, *J. Geophys. Res., 95*, 18,095–18,110, 1990.

Pollard, R. T., and L. A. Regier, Vorticity and vertical circulation at an ocean front, *J. Phys. Oceanogr., 22*, 609–625, 1992.

Rosenfeld, L. K., and R. C. Beardsley, Barotropic semi-diurnal tidal currents off northern California during the Coastal Ocean Dynamics Experiment (CODE), *J. Geophys. Res., 92*, 1721–1732, 1987.

Siegel, D. A., T. D. Dickey, L. Washburn, M. K. Hamilton, and B. G. Mitchell, Optical determination of particle abundance and production variations in the oligotrophic ocean, *Deep Sea Res., Part A, 36*, 211–222, 1989.

Smith, R. C., K. J. Waters, and K. S. Baker, Optical variability and pigment biomass in the Sargasso Sea as determined using deep-sea optical mooring data, *J. Geophys. Res., 96*, 8665–8686, 1991.

Stegmann, P. M., M. R. Lewis, C. O. Davis, and J. J. Cullen, Primary production estimates from recordings of solar-stimulated fluorescence in the equatorial Pacific at 150°W, *J. Geophys. Res., 97*, 627–638, 1992.

Stramska, M., and T. D. Dickey, Variability of bio-optical properties of the upper ocean associated with diel cycles in phytoplankton population, *J. Geophys. Res., 97*, 17,873–17,887, 1992.

Strub, P. T., P. M. Kostro, A. Huyer, and CTZ Collaborators, The nature of the cold filaments in the California Current system, *J. Geophys. Res., 96*, 14,743–14,768, 1991.

Swenson, M. S., P. P. Niiler, K. H. Brink, and M. R. Abbott, Drifter observations of a cold filament off Point Arena, California, in July 1988, *J. Geophys. Res., 97*, 3593–3610, 1992.

Washburn L., D. C. Kadko, B. H. Jones, T. Hayward, P. M. Kosro, T. P. Stanton, S. Ramp, and T. Cowles, Water mass subduction and the transport of phytoplankton in a coastal upwelling system, *J. Geophys. Res., 96*, 14,927–14,945, 1991.

Zaneveld, J. R. V., An asymptotic closure theory for irradiance in the sea and its inversion to obtain the inherent optical properties, *Limnol. Oceanogr., 34*, 1442–1452, 1989.

M. R. Abbott, College of Oceanic and Atmospheric Sciences, Oregon State University, Corvallis, OR 97331. (e-mail: mabbott@oce.orst.edu)

D. Blasco, 102 De Sept Lacs, St. Donat, Rimouski, Quebec, Canada G0K 1L0.

C. R. Booth, Biospherical Instruments, Inc., 5340 Riley Street, San Diego, CA 92110.

K. H. Brink, Woods Hole Oceanographic Institution, Woods Hole, MA 02543.

L. A. Codispoti, Office of Naval Research, Code 3241, 800 N. Quincy Street, Arlington, VA 22217.

C. O. Davis, Naval Research Laboratory, Code 7212, 4555 Overlook Ave. SW, Washington, DC 20375.

M. S. Swenson, Atlantic Oceanographic and Meteorological Laboratory, NOAA, 4301 Rickenbacker Causeway, Miami, FL 33149.

(Received November 30, 1993; revised September 7, 1994;
accepted September 14, 1994.)